A COMPARISON OF MICROPLASTIC STRAIN PRODUCED STATICALLY AND DYNAMICALLY

Thesis by

Oliver A. Baer

In Partial Fulfillment of the Requirements for the Degree

of Mechanical Engineer

California Institute of Technology

Pasadena, California

1948

ACKNOWLEDGMENT

This investigation was carried out under the general supervision of Dr. D. S. Clark of the California Institute of Technology, to whom thanks are hereby extended for his advice, assistance, and interest in the investigation. Thanks are also extended to Dr. P. E. Duwez for the annealing of the specimens and his interest in the problem.

The impact machine employed is the property of the Mechanical Engineering Department of the California Institute of Technology, having been built in 1939 for the investigation of impact properties of metals.

Funds for the material tested and for modification of the impact machine were provided by David Taylor Model Basin, Navy Department, Washington, D. C., through Navy Contract NObs - 34183, Task Order 3.

ABSTRACT

The object of this investigation was the microscopic comparison of the structure of alpha brass resulting from strain produced statically and dynamically. The dynamic strain was produced at an impact velocity of 150 ft/sec.

It was observed that for the same strain produced at the two rates of loading, there was no observable difference in the resulting microstructure. The strains varied from 1.3 percent to 10.9 percent. For this same range of strain, it was also observed that except for the apparent amount of slip on each individual slip plane and the distortion of the surface, the resulting microstructure was practically independent of the amount of strain.

In the grains which had only one slip system acting and in which the slip lines were distinct enough so that a count could be made of them, the average spacing of the slip lines was about 0.6 micron, varying from a minimum of 0.38 to a maximum of 1.0 micron. The slip line spacing for grains in which more than one slip system was acting appeared to vary from 0.4 to 4 or 5 micron.

Approximately 40 percent of the grains observed had two slip systems acting, and this percentage did not vary appreciably with strain. Not enough grains were found with three systems of slip acting at the same point to form any valid conclusion concerning this phenomenon. At least 95 percent of the grains showed slip lines, even at the smallest strains observed.

No conclusions could be made concerning the possibility of twinning in the deformation of alpha brass, except that it is certain that no large mechanical twins are produced. Twinning in this material is still a controversial issue, and its detection involves more elaborate investigation.

TABLE OF CONTENTS

INTRODUCTION

A. The Mechanism Of Plastic Deformation

In general, plastic deformation takes place by two fundamental mechanisms, slip and twinning. In some materials, however, the deformation takes place by only one of the two processes. For example, it appears that metals with a body centered cubic structure deform only by slip, while some particular metals of other structures deform only by twinning when they are carefully tested. Under certain conditions the method of deformation may change. Ferrite, for example, deforms only by slip when subjected to tension at room temperature; but under impact conditions or at low temperatures, deformation occurs also by twinning, forming the well-known Neumann bands. Other metals such as bismuth and antimony, that deform only by twinning when they are tested in tension at room temperatures, exhibit slip lines when they are tested in compression or in tension at higher temperatures.(1)*

In alpha brass, slip takes place on the $\{111\}$ planes, as it does in most face centered cubic structures. When the distortion occurs under unusual circumstances such as by impact loading or at very high or very low temperatures, the slip may take place on other than the $\{111\}$ planes. In other materials, the slip takes place on planes characteristic (2) of the material, the structure, and the method of deformation.

*Numbers in parentheses refer to articles listed in the bibliography.

The twinning plane in α-brass is also the $\{111\}$ plane, the plane of densest atomic packing. This twinning is produced by annealing, and not by deformation. To attempt to show that mechanical twins are also found in deformed copper, Mathewson (3) in 1928 reported that the twins inside recrystallized grains were more apt to be parallel to the prior slip lines in these grains, and he proposed that some of what were thought to be slip lines were twins. This proposition by Mathewson was substantiated in 1934 by Samans (4) who showed by X-Rays the possibility that in deformed single crystals of copper, there were some regions that were twinned mechanically. In view of the fact that there has been considerable difference of opinion as to whether deformation twins are produced in brass and copper, it is unfortunate that no one has either substantiated Samans' observation or used his method (the Davey - Wilson method) to refute his arguments.

While the slip planes and twinning planes in brass are of the same form, the direction of movement is different in the two processes. In slip, the movement of the atoms takes place in the $[10\bar{1}]$ direction. In the process of twinning, the movement is in the $[11\bar{2}]$ direction.

In the process of deformation, it has been shown (5) that in α-brass it is at least very doubtful that twinning occurs. If there is any twinning, however, the twins should appear parallel to the slip lines, from which they would have to be distinguished. Moreover, the twins would be of the same order of magnitude of length and thickness as the space between the slip lines, and it is doubtful that they could be observed with the ordinary microscope. On the other hand, when a specimen of polycrystalline brass is deformed, the slip lines appear in definite patterns on a polished surface of that material. The appearance of the slip lines is different for different materials, however, and is even different for single crystals of brass as compared with polycrystalline brass.

In polycrystalline brass the lines which form the pattern appear simultaneously in the grain, and as the deformation is increased the pattern of lines remains the same. In a single crystal of brass, the initial strain appears as a thin band of lines, and as the strain is increased, this band of lines merely becomes wider, maintaining the same density of slip lines.(6)

Wheras in brass the slip line spacing may be constant with strain, in some other materials more slip lines may appear between the original ones as the strain is increased. In aluminum, for example, more slip lines appear as a function of the strain with such regularity (2) that if a plot is made relating the strain and the number of slip lines, a very smooth curve results.

When the slip lines appear in brass, they appear in a pattern that depends on the shape of the crystal, its orientation, and the influence of the surrounding grains. The lines naturally follow the atomic planes through a twinned region and thus appear as jagged lines in regions of annealing twins. They also appear, more generally in larger grains, in crisscross patterns showing that movement has taken place on more than one slip system. In these cases the slip lines are considerably farther apart than in the cases in which only one system is in operation. In copper, the spacing of these lines varies widely, being of the order of 0.3 micron for the closest spacing (7), and up to 6 or 8 microns for these crisscross patterns. Also in the case of these crisscross patterns it is generally true that the displacement in the center of the grain is much more than it is at the edge, indicating the rigidity of the grain boundary region. Aston (8) measured the difference in displacement from the edge to the center of the grain. But since his investigation was on a specimen with very large grains, his results may be interpreted only qualitatively when a study of polycrystalline material is made.

When the planes of the brass crystal slip relative to each other, the grain boundaries must also deform because of the continuity of the system. This produces severe localized stress on the neighboring crystal, causing it to deform plastically. So in this way the plastic strain is transmitted throughout the material, and an explanation of why so many of the grains have slip in them is presented.

The slip that takes place within the crystal deforms the individual crystals. The cumulative effect of the distortion of all the grains is then the distortion of the polycrystalline specimen, which may be observed macroscopically.

B. Static Versus Impact Loading In Relation To Plastic Deformation

Extensive investigations have been made to study the properties of materials when tested under impact conditions (9,10,11), and it has been found that in general the apparent stress-strain curve is much higher, and that also the total elongation possible before rupture is greater. Also considerable study has been made of the structure resulting from plastic deformation (12). However very little specific correlation between high rates of strain and the resulting microstructure has been offered.

It has been found (13) that impact is more conducive to twinning for certain materials, notably the body centered structures. On the strength of this it was expected that impact would also produce twinning in face centered cubic structures. In 1928 Mathewson (2) suggested this, but admitted that the possibility was only apparent. What was thought to be twins were some lamellae which appeared very much like the Neumann bands in iron. Lower rates of strain produced very few of these lamellae, so it was assumed that they were twins. The reason that impact conditions are favorable to twinning, hypothesized Mathewson, was that under this type of loading a given small displacement is momentarily distributed among many planes, thus disturbing the equilibrium of large numbers of atoms and potentially favoring the formation of sizeable twin bands.

Subsequently, however, Mathewson and Van Horn (14) attempted to produce a large mechanical twin in a single crystal of copper by constraining the specimen so that the $\{111\}$ planes would move relative to each other in the $[11\bar{2}]$ direction. All attempts to produce any deformation in this direction were unsuccessful, however, so they admitted that the possibility of twinning in face centered cubic structures was very small.

In view of the fact that the properties of metals are considerably different when tested at different rates of strain, it is reasonable to ask if the differences in the properties may not be related to a difference in the mechanism of plastic deformation, resulting in different slip patterns when the same material is tested at markedly different loading rates.

The purpose of this investigation, then, was to find whether there is any observable difference between the microstructure produced by impact and the microstructure produced by static loading.

C. Results Of Previous Pertinent Investigations

In 1937 Andrade and Roscoe (15) found that the slip line spacing in lead was quite uniform, giving a probability distribution of spacings around a value of approximately 4 microns. They found that this spacing was not affected by small changes in temperature ($0^{\circ}$to $100^{\circ}C$), by the size or shape of the crystal, or by the amount of strain, contrary to the results found for aluminum. Also they reported that there was no significant change of spacing with different rates of straining; but since their maximum rate of strain was only 3 in./in./sec, this fact has little significance in the present investigation.

The work of Andrade and Roscoe is significant in that it subtly indicates why there is so little data offered on slip line spacing. They observed a spacing of about 4 microns, which is very easily resolved under the microscope, wheras most other metals have a spacing much smaller than this, and indeed very near the resolving power of the ordinary microscope. This fact undoubtedly limited the observations on aluminum.

In recent years, the difficulties due to the limited resolving power of the ordinary microscope have been overcome by the increasing use of the electron microscope in metallurgy. Several investigations of structure have been reported (7, 16, 17), and these included slip line spacings, but unfortunately neither brass nor aluminum was included.

In one of these papers, however, Barrett (7) did give the spacings found for polycrystalline copper. The spacings varied from 0.25 microns to more than 2 microns, with no predominance of any particular spacing. Even if all the spacings were exactly the same throughout the specimen, it would not be expected that the spacings would appear the same on the surface observed, but at least there would be a predominance of smaller apparent spacings. So it is apparent that the slip planes do not have the same spacing from grain to grain, although the spacing is quite constant within any one grain.

In 1944, Parker and Smith (18) published the results of some tests they performed on single crystal and polycrystalline copper to show the difference in properties when that material was tested statically and dynamically. Upon examination of the microstructure of the single crystals, a considerably closer spacing of the slip lines when the material was tested at high velocities (100 ft/sec) than resulted from static testing. They also took electron micrographs of the surface after the strain, and found that the higher velocities produced broader regions around each slip line affected by the strain. This observation was on single crystals in which the orientation of the structure was different in each test. Since the spacing of the lines and the resulting surface is very dependent on the orientation of the crystal with respect to the applied force, it is quite possible that their observations are markedly influenced by this fact.

Unfortunately, Parker and Smith did not examine the microstructure of the polycrystalline specimens. Some electron micrographs of this structure would have been very enlightening.

EXPERIMENTAL INVESTIGATION

A. General Procedure

A valid comparison between statically tested and dynamically tested specimens can only be made on the basis of observations of regions strained the same amount in the two specimens. The means by which the desired amount of strain is produced at a given velocity of impact must therefore be investigated.

As is shown in Appendix I, the strain is a function of the velocity of impact, the point of the specimen under consideration, and the time after the moving end of the specimen is initially struck, as well as the stress-strain diagram for the material. By adjusting the distance through which the moving end of the specimen may travel, the desired strain can be produced at a given point of the specimen, for a given velocity of impact.

The theoretical calculation of the strain distribution, however, takes into account some simplifications which are not possible in the actual production of the strain under impact loading. The first is the assumption of complete rigidity of all the parts of the machine producing the impact, so that the moving end of the specimen may be instantaneously accelerated to the impact velocity. This is clearly a great simplification. Another assumption made is that the stress-strain curve does not change with the rate of loading.

Although the machine employed for the impact by no means meets the requirements of the theory, and it is known that the dynamic stress-strain curve is much higher than the static curve, the theory presented in the appendix gives a good first approximation to the resulting strain distribution.

The procedure consisted of first calculating the distance through which the moving end of the specimen must move to produce a given strain at a given point in the specimen, all for the desired velocity of impact. Then the specimen was tested dynamically and the strain measured. Subsequently another specimen was strained statically to the same strain as appeared at the point under observation in the dynamic specimen.

After the two specimens were thus strained the same amount at the point of comparison, one tested statically and one tested dynamically, the resulting microstructures were compared by photographic and visual means.

B. Material Investigated And Preparation Of The Specimens

The material investigated was cartridge brass, 70 percent copper and 30 percent zinc. It was obtained in the half-hard condition as a 1/8 in. sheet, 18 in. by 96 in. Since all the specimens were cut from this same piece of stock, it was assured that they were all of the same composition and initial condition. The specimens were made as shown in Fig. 1, the test section being 1/4 in. x 1/8 in. in cross section and 8 in. long. The area of the cross section chosen was small enough so that the specimen could be tested with the equipment at hand, but the specimen was still wide enough so that the surface could be polished electrolytically. The 8 in. dimension was chosen because it has been found in studies of the influence of specimen length on the strain distribution in tensile impact testing (19) that an 8 in. specimen was the shortest, for the cross section chosen, in which the strain distribution was consistent and could be fairly accurately predicted.

The specimens were finish machined and then annealed at 1200 °F for 1 hour in dry hydrogen. The resulting mean average grain diameter was approximately 0.06 m m.

Subsequent to the anneal, one side of the specimens to be tested under impact loading were marked with scratches every 0.10 in. along the length. The spacings of these scratches were then measured to .0001 in. by a comparator employing a low power microscope. Subsequent to the test, the spacings were again measured, and compared with the original values. Since the scratches were

0.10 in. apart originally, the difference in milli-inches between the original and the final spacing gave the percentage of strain directly. Because of the inaccuracies of measurement, the errors in spacing difference may have been as much as .0005 in., but since the strain is continious from one element to the next, a plot was made of the strain in each element versus its position along the specimen, and a smooth curve approximating all the points obtained gave the actual strain distribution very closely. Strain distribution diagrams are presented in Appendix II.

To determine the strain in the specimens to be tested statically, two points were marked 15 cm apart on the gage length. Then after straining in a static testing machine the distance between the two original points was again measured and the resulting strain directly calculated.

After scratching and measuring the original distances between the scratches, the specimens were cleaned with fine abrasive cloth and polished electrolytically on the side opposite to the scratches. Eight spots were polished along the length of the dynamic specimes, since each spot would have a different strain upon testing. Since the strain in the static specimens was constant throughout the length, only two or three spots were polished.

With the completion of the scratching and polishing treatments, the specimens were ready for testing.

C. Dynamic Tests

1. Description of the Equipment

Fig 2 is a sketch of the essential features of the impact testing equipment employed, except that the means of propulsion for the hammer which strikes the specimen is not included. Fig. 3 is a photograph of the machine cocked for a test, with the specimen in place.

In Fig. 2, the specimen (A) is fastened rigidly with dowel pins to the upper grip (B), which is in turn screwed into a piece of Shelby tubing (C) suspended from the top of the machine. This supporting tube is 10 ft long. The bottom end is pinned to the lower grip (D), but is pinned in such a way that the pins may slide freely in slots in the lower grip. The reason for these slots will be given shortly. A phosphor bronze shearing disc (E) is fastened to the lower grip by a nut (F). A circular groove is machined in this disc so that the part of the disc outside the groove will shear off at the proper instant during the test. The edges of this disc are notched in two places, and these rectangular notches are engaged by the rails (G) on which the hammer (H) travels. The notches are so arranged on the shearing disc that when they engage the rails, the bottom end of the specimen assembly is centered between the rails.

The hammer is propelled downward by six heavy rubber bands; these bands have a cross section of 3/8 in. by 1 in. The hammer is released from a height of approximately five feet above the specimen, being elevated to this initial position by a sprocket and chain arrangement driven by a motor on top of the machine. The hammer

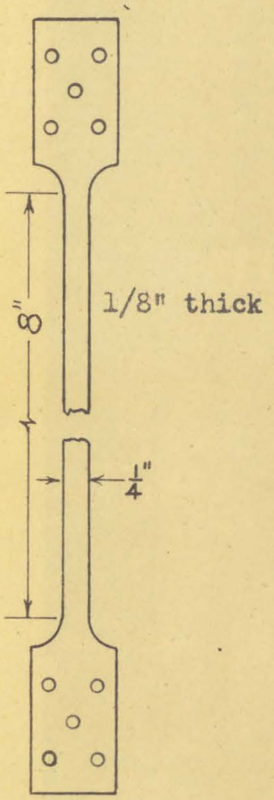

Fig. 1
Tensile Impact
Test Specimen

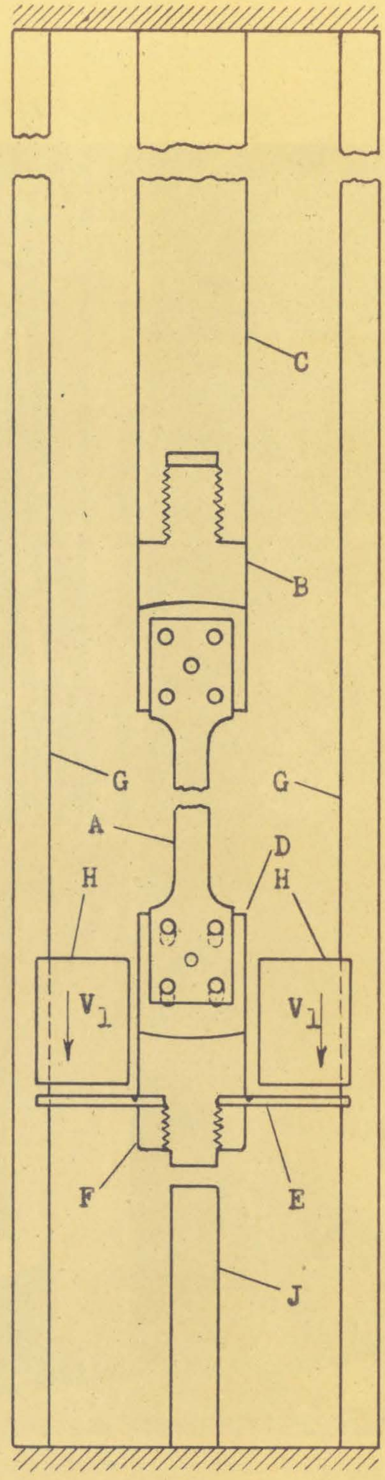

Fig. 2
Impact Testing Machine

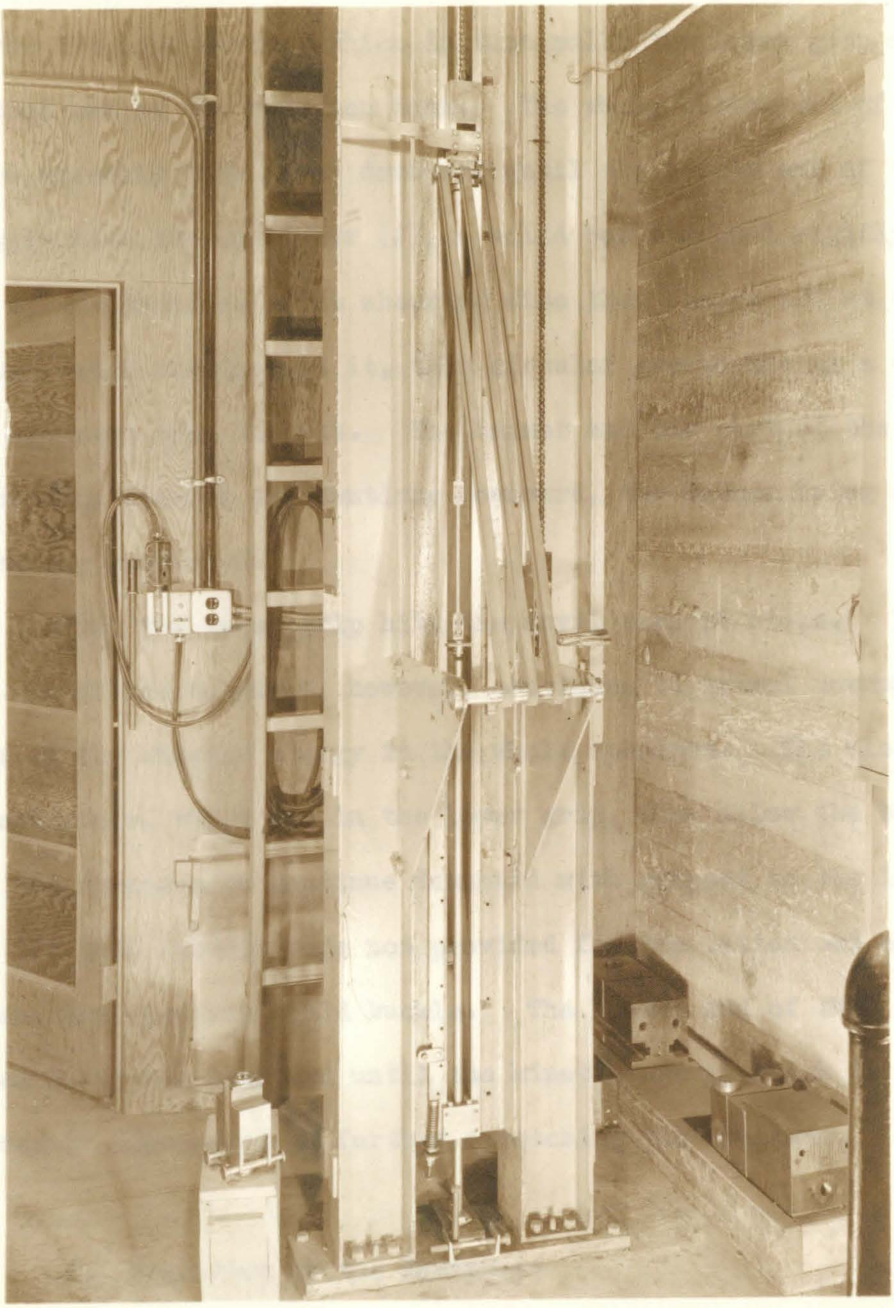

Fig. 3 Impact Testing Machine, Showing Specimen
in Position for Test

has a hole in the center of it so that it can pass down over all the assembly except the shearing disc. When it strikes the shearing disc, it starts the disc mvoing, which in turn pulls the lower grip and the bottom end of the specimen down. The whole bottom end of the specimen assembly than moves downward until the bottom end of the lower grip hits the anvil bar (J), a solid bar attached rigidly to the bottom of the machine. The shearing disc then shears off at the circular groove machined in it, this circular groove having a slightly larger diameter than the nut. The hammer and the part of the shearing disc that has sheared off continue downward, the hammer being caught by a braking mechanism.

When the lower grip hits the anvil bar, it stops. The bottom end of the specimen, however, continues to travel downward because of the kinetic energy in the whole specimen. The slots mentioned above, which are in the lower grip, then allow the bottom end of the specimen to continue downward with respect to the lower grip. If this freedom were not provided for the bottom end of the specimen, the specimen would buckle. The bottom end of the specimen continues downward until the kinetic energy which it possesses is dissipated in further stretching the specimen.

2. Operation of the Equipment

The two variables which can be controlled to produce the desired strain distribution are the velocity of impact and the distance that the lower grip travels before it hits the anvil bar.

The velocity of the hammer is measured by means of electrical contacts mounted on a strip attached to the rails. A finger is attached to the hammer which engages these contacts momentarily as it travels by. There are five of these electrical contacts, and they are all part of a circuit which includes a voltage supply, an amplifier, a single sweep generator, and an oscilloscope. When the hammer passes by and the finger engages the first contact, a sweep is initiated in the single sweep generator and applied to the horizontal axis of the oscilloscope. The sweep is of such duration that the finger engages all the other four contacts during the course of the sweep. The other contacts are so arranged in the circuit that as each is engaged by the finger, a momentary pulse of voltage is applied to the oscilloscope through the amplifier, causing the spot on the oscilloscope to deflect vertically. But as the spot is in the process of moving horizontally across the screen as each of these four contacts is engaged, the resulting horizontal sweep has four momentary displacements in it. This sweep is photographed as it occurs.

Subsequently, another sweep of the same duration is applied to the oscilloscope, but this time with timing markers from a variable frequency oscillator superposed on it. The time between timing markers on this sweep is known, so the time elapsing between the displacements in the first sweep are obtained directly by comparison. The time required for the hammer to travel past the four velocity contacts is then known, and since the distance between the velocity contacts is known, the velocity of the hammer follows directly.

The velocity of the hammer is controlled by the height above the specimen from which it is released. A hammer of 3 3/4 lb was used in the tests.

The total elongation of the specimen is controlled by varying the distance through which the lower grip travels before it hits the anvil bar. This is done by placing steel blocks under the anvil bar to block it up. The anvil bar is held in a guide a few inches above the base to align it with the lower grip. A soft copper sheet is placed under the anvil bar to absorb some of the shock. Also a copper disc is placed between the lower grip and the anvil bar so that the elastic rebound of the lower grip as it strikes the anvil bar is minimized.

3. Testing Procedure

It was first necessary to decide the velocity at which a range of strains was to be investigated. Since the greatest change of microstructure from that produced statically should come at the maximum velocity attainable with the equipment, it was decided to investigate a range of strains at that velocity. The maximum velocity attainable was 150 ft/sec.

In the testing program, the velocity was not measured each time; instead the hammer was released from the same height each time. Several preliminary tests were made to determine if the velocity could be determined accurately by the height from which the hammer was released, and it was found that the velocity varied less than

2 percent over several tests from the same height. The calibration curve of velocity versus the height from which the hammer was released is presented in Appendix III.

As is shown in Appendix I, a velocity of 150 ft/sec produces an initial maximum uniform strain of 12.3 percent near the moving end of the specimen, provided the duration of the impact is short enough so that the plastic waves reflecting from the fixed end of the specimen do not have time to propagate the length of the specimen and increase the strain near the moving end. The strains at points other than adjacent to the moving end of the specimen are determined entirely by the total amount of elongation produced in the specimen. Since a strain of 12.3 percent is uniquely determined by a velocity of 150 ft/sec, and any other strain up to 12.3 percent theoretically also can be attained, it was decided that the range of strains from 0 to 12.3 percent should be investigated at a velocity of impact of 150 ft/sec.

Tests were performed with the total elongation of the specimen varying between 0.21 in. and 0.52 in. This total elongation is the distance between the lower grip and the anvil bar plus the additional strain produced in dissipating the kinetic energy of the specimen. The distance between the lower grip and the anvil bar was 0.05 in. in the case where 0.21 in. total elongation resulted, and was 0.30 in. in the case where 0.52 in. total elongation resulted. The minimum strain produced in the case of the 0.21 in. elongation was 1.3 percent; the minimum strain produced in the case of the 0.52 in elongation was 4.3 percent and the maximum strain in this case was 11.2 percent. The region in which the 11.2 percent strain occurred was not polished, however, so the microstructure could not be examined. The maximum strain at which the microstructure was examined was 10.9 percent and the minimum strain at which the microstructure was examined was 1.3 %. Three specimens were tested at 150 ft/sec for the slip line comparison and one was tested at 135 ft/sec for observation of twins. In one of the specimens, the resulting microstructure was examined at strains of 4.8, 6.6, 8.8, and 10.9 percent. In two others, the strain was examined at 2.4 percent in one and 1.3 percent in the other. The structure in the specimen tested for twinning observation was examined at a strain of 4.3 percent.

D. Static Tests

After the strain distribution each of the dynamic specimens was determined, it was necessary to statically strain other specimens to the same amount of strain appearing in each of the regions of the dynamic specimens to be investigated. Each static specimen was then prepared for the test, and strained in a small (3000 lb) testing machine until the desired strain resulted. It was necessary that each static specimen be strained enough so that after the elastic recovery of the material, the desired strain would result.

To correspond to the strains in the dynamic specimens which were to be investigated, one specimen was strained statically to each of the following strains: 1.3, 2.4, 4.8, 6.6, 8.8, and 10.9 percent.

E. Method Of Comparing The Microstructures

The first object of the investigation was the determination of whether any twins were produced mechnically that could be detected by microscopic means. A specimen was prepared for a dynamic test as described, and was also etched so that the annealing twins were discernable. A particular region was then photographed, and subsequently the specimen was tested at an impact velocity of 135 ft/sec. After testing, the same region that was originally photographed was examined visually and photographed again. Then the spot was repolished and re-etched so that any new twins which may have been produced by the impact test could be observed. It was again examined visually and photographed. The repolishing and re-etching were necessary because the strain in the material produced a distortion of the surface, making it difficult to focus for the photograph; also another etch applied to the already etched region would have left it so dark that small twins would have been obliterated by the etch.

For the comparison of the slip line characteristics, preliminary tests were made to determine what features of the microstructure were to be observed and compared. It was found upon statically straining a specimen to 5 percent strain that the grains fell into four general classes, depending on the structure in them. The first class of grains were those in which there was only one slip system acting, the slip lines being fairly uniform and distinct throughout the grain. In these grains, the comparison to be made concerned the average spacing of the slip lines throughout the grain. The second class included those grains in which there was more than one slip system acting. The comparison to be made concerning this class of grains was the percentage of grains in which this structure occurred. The third class included those grains in which slip lines were observed, but the lines were not sufficiently distinct to permit counting. The fourth class was composed of those grains in which no slip lines were visible. The comparison to be made concerning the third and fourth classes was the percentage of these grains appearing. Examples of these classes of grains are shown in Fig 4. The first class is shown at (1) the lines being uniform and constant across the grain. The second class is shown at (2a), (2b), (2c).

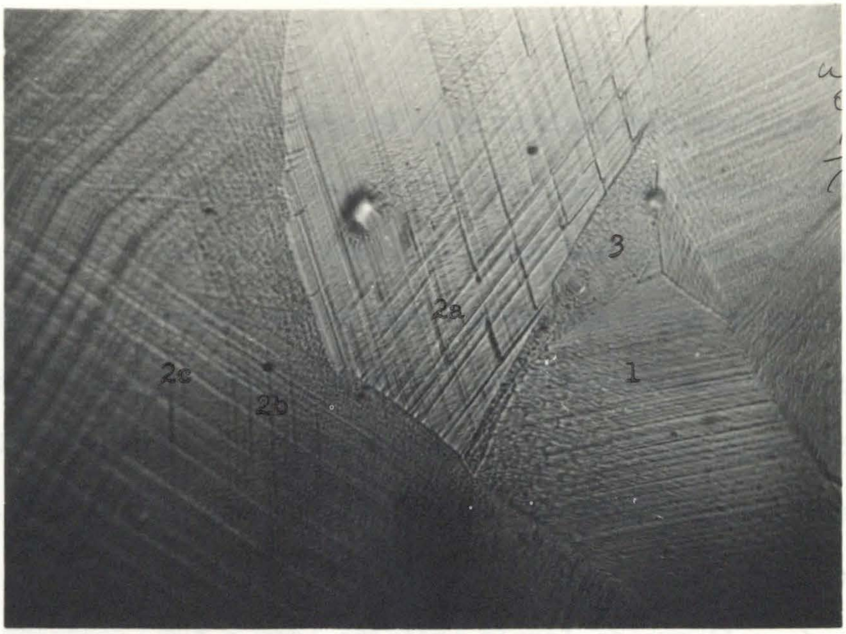

Fig. 4 Photomicrograph Showing Typical Slip Line Patterns
Magnification: 900x; Static Strain: 5.0%

Fig.5 Photomicrograph of Typical Area Analysed in Making Slip Line Investigation. Mag: 150x
Strain: 4.8% Impact Velocity: 150 ft/sec

At (2a) there are two systems of slip acting, but the lines are not uniform across the grain, indicating that prisms of material have slipped out of place. At (2b) are shown two systems of slip which are apparently independent of each other, the lines in each set being unaffected by the other set. At (2c) is shown a region in which three systems of slip are acting. The third class of grain, that in which slip lines were observed but could not be counted, is shown at (3). The slip lines in this grain can not be seen in this photomicrograph, but a more exacting visual observation showed that they were actually present. There were very few grains in which no slip lines occurred, and none appear in this photomicrograph.

The procedure of determining the comparison was as follows: Subsequent to straining the specimen, one photomicrograph of the resulting structure was made at a magnification of 150 x. The resulting structure appeared as in Fig. 5. As is evident from this photomicrograph, the grain boundaries are quite indistinct. The same region photographed was then located under the microscope, where the grain boundaries were easily distinguishable, and lines representing the actual grain boundaries were superposed on the photomicrograph. For the grains in which a count could be made of the slip lines, the number of lines was marked directly on the picture, together with the two points in the grain between which the lines were counted. From the number of lines, the distance between which they were counted, and the magnification of the photomicrograph, the actual spacing of the slip lines could be directly calculated. The magnification of 150 x was checked by measuring on the ground glass of the metallograph the image produced from a stage micrometer, using the same objective, ocular, and bellows extension as were used for the actual photographs. The grain boundaries were determined at a magnification of 500 x and the individual analysis of each grain, including the number of slip lines contained in the first class of grains, was made at a magnification of 1400 x with an objective having a numerical aperture of 1.3.

From the preliminary tests it was observed that there were quite a number of very small grains throughout the structure, mostly at the intersections of three large grains. Because of the rigidity of the grain boundaries, the constraints on these smaller grains were much greater than the constraints on the larger grains, so it was desired to exclude the small grains from the investigation. If the grain was so small that a good representation of its boundary could not be drawn with pen and ink on the photomicrograph, it was excluded. This excluded all the grains of a mean average diameter of less than about 0.015 m m.

Other observations concerning the slip lines were made which could not be expressed quantitatively. These observations were on the straightness of the slip lines and other general appearances, whether or not the lines were more predominant toward the center of the grain, and how the lines were affected by twinned regions and neighboring grains.

F. Experimental Results

Figs. 6, 7, 8 are photomicrographs taken at various stages in the history of a specimen strained dynamically to 4.3 percent at this particular point. The impact velocity was 135 ft/sec. Fig. 6 shows the original condition of the structure after polishing and etching to reveal the annealing twins. Fig. 7 shows the same region subsequent to the test, and Fig. 8 the same region after repolishing and etching. If any large twins were produced as a result of the impact test, they would appear as new regions in Fig. 8 which were not present in Fig. 6, the original condition. The same regions photographed were also examined visually so that a better observation could be made. No twins were observed which were not present in the original structure.

No further investigation was made photographically of the possibility of twinning, but during the course of the slip line observations a check was made several times on regions which appeared as if they may have been twinned mechanically. These areas were etched to see if they would color preferentially in comparison with the rest of the structure. But in no case were there any small regions found which could be shown to be mechanical twins.

Upon analysis of the slip line characteristics by the method described, the results were compiled and are presented in Fig. 9 and in Tables I and II. As shown in Table I the average spacing found in any one grain, for all the six strains considered,

Fig. 6

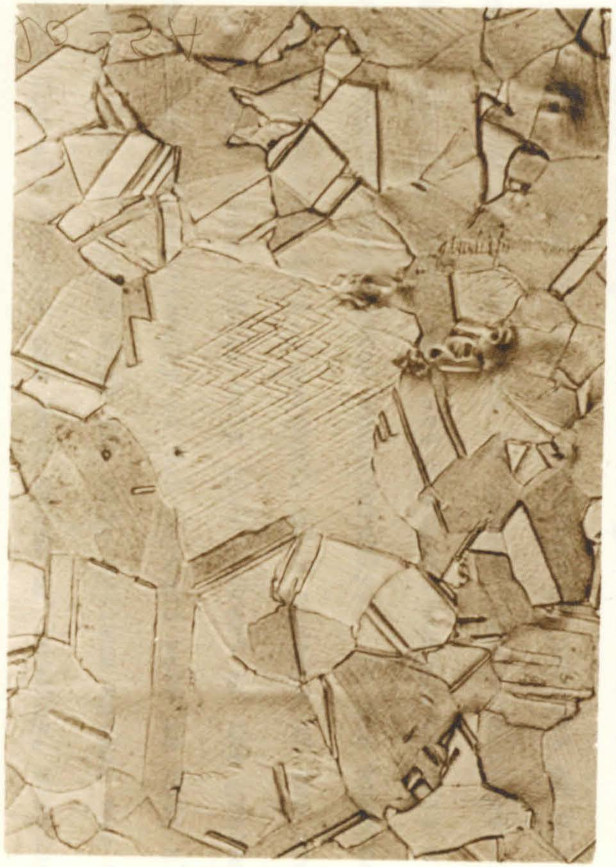

Fig. 7

Fig. 8

Fig. 6 Typical Region Etched to Show Annealing Twins. Mag: 400x

Fig. 7 Same Region as Fig. 6, Subsequent to Strain of 4.3% at Impact Velocity of 135 ft/sec.

Fig. 8 Same Region as Fig.7, but Repolished and Etched.

Etchant Used: 1 part H_2O_2, 5 parts conc. NH_4OH, 5 parts water.

varied from a minimum of 0.39 micron to a maximum of 1.00 micron. The mean average spacing for all the grains counted in any one photomicrograph varied from a minimum of 0.51 micron in the case of the region strained 4.8 percent dynamically to a maximum of 0.67 micron in the cases of 8.8 and 10.9 percent strain produced dynamically and the case of 8.8 percent static strain. At least 16 determinations of the slip line spacing were made for each strain. Table II shows the comparison of the general characteristics of the slip lines. It was found that at least 95 percent of all the grains observed had slip lines in them. The percentage of grains in which the slip lines were not distinct enough so that a count could be made of them varied considerably. In the specimen statically strained to 1.3 percent, 60.1 percent of the grains fell into this class, while only 19.4 percent of the grains in the specimen strained statically to 8.8 percent were in this class. The percentage of grains with two slip systems acting was quite constant for all strains and both rates of loading, varying from 35.2 percent to 51.0 percent. A rough count was made on several of the grains in which there was more than one slip system acting, and it was observed that the spacings in this type of grain varied from 0.4 micron to approximately 5 micron.

There were several regions in each area observed in which there were three systems of slip acting, but not enough of these regions to obtain results which would be valid statistically. These regions generally appeared in a grain which would normally

Fig. 9a

For the particular area indicated, and for the total number of grains in this area in which the slip line spacing was determined (e.g., for the 27 grains, 10.9% strain, static test), the percentage of this class of grains with a spacing between the limits indicated is plotted against the spacing.

A. 10.9% Strain

1. Tested at 150 ft/sec
   45 Spacing determinations
   Ave. spacing: 0.68 micron

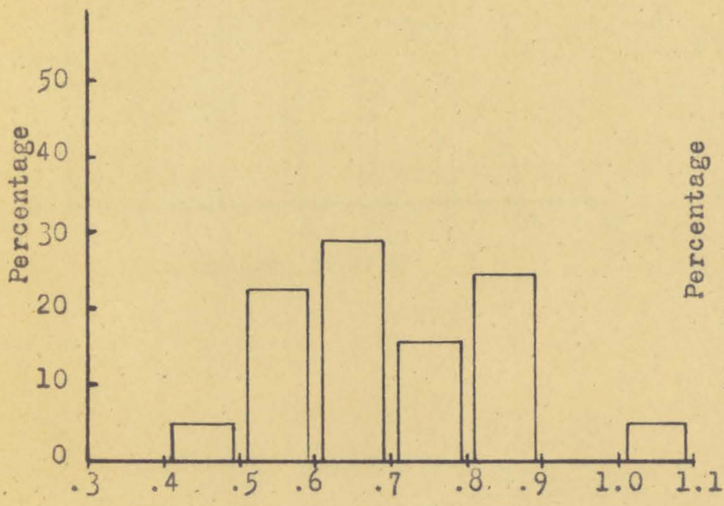

2. Tested statically
   27 spacing determinations
   Ave. spacing: 0.62 micron

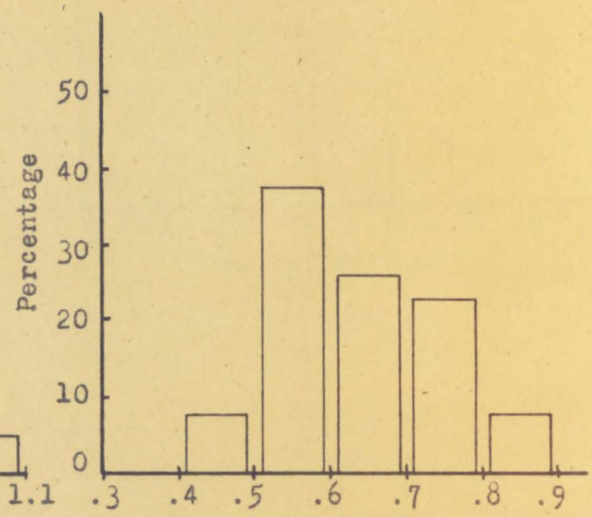

B. 8.8% Strain

1. Tested at 150 ft/sec
   16 Spacing determinations
   Ave. spacing: 0.67 micron

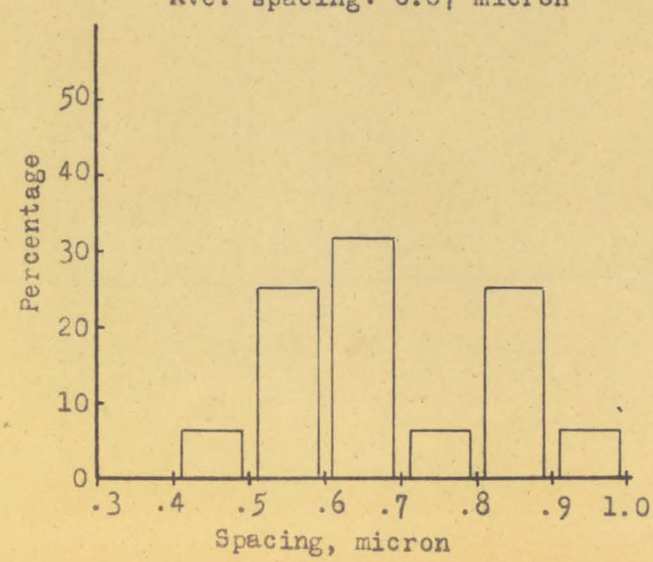

2. Tested statically
   33 spacing determinations
   Ave. spacing: 0.67 micron

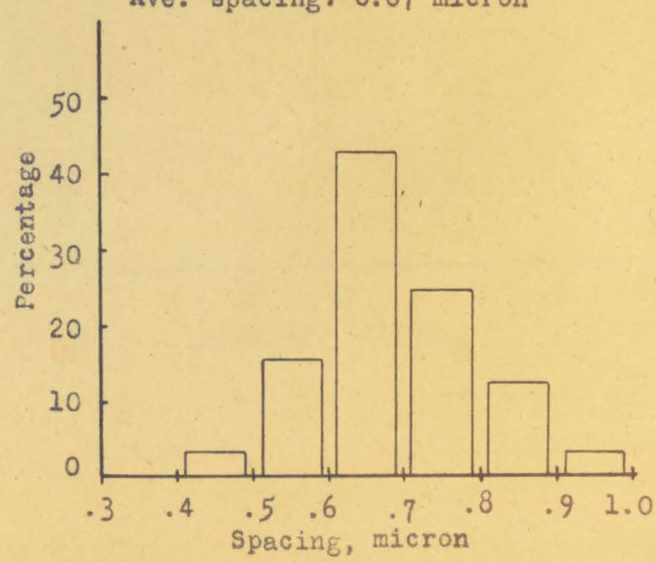

FIG.9b

C. 6.6% Strain

1. Tested at 150 ft/sec
17 Spacing determinations
Ave. spacing: 0.60 micron

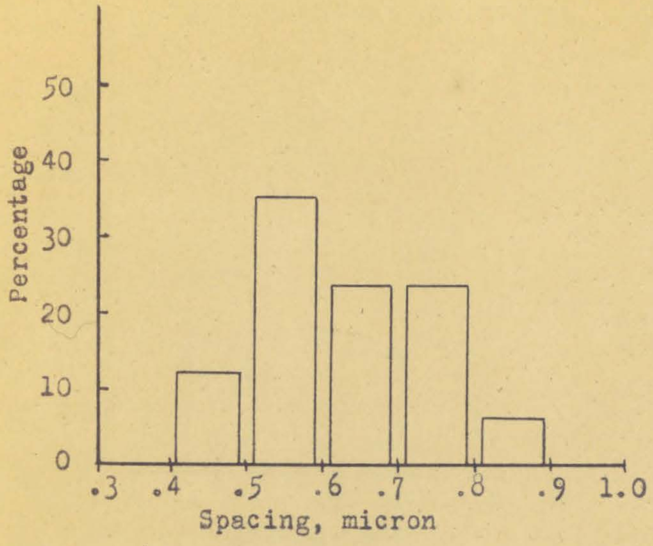

2. Tested statically
25 Spacing determinations
Ave. spacing: 0.56 micron

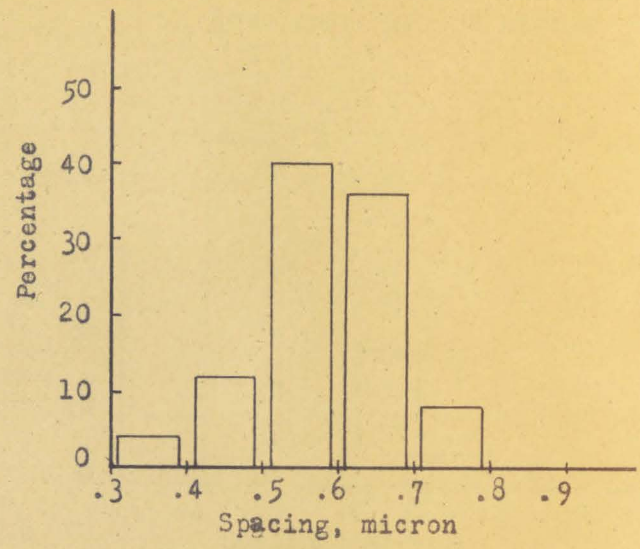

D. 4.8% Strain

1. Tested at 150 ft/sec
24 Spacing determinations
Ave. spacing: 0.51 micron

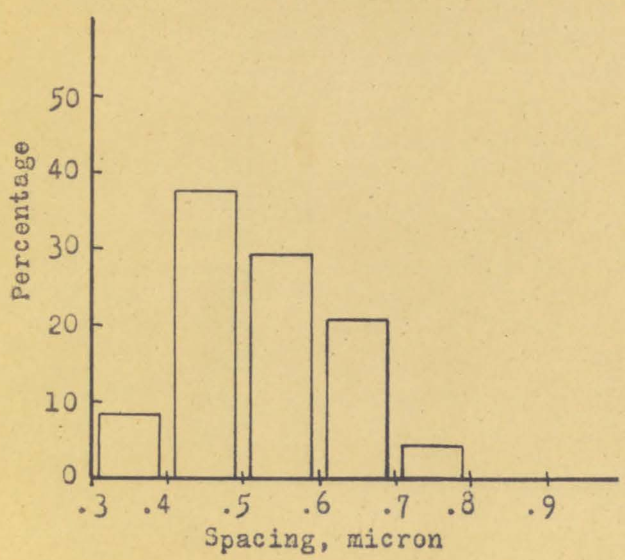

2. Tested statically
27 spacing determinations
Ave. spacing: 0.57 micron

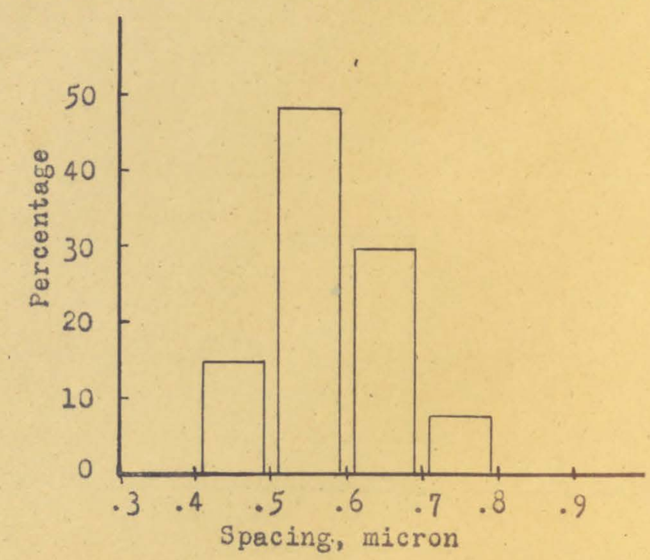

Fig. 9c

E. 2.4% Strain

1. Tested at 150 ft/sec
19 Spacing determinations
Ave. spacing: .56 micron

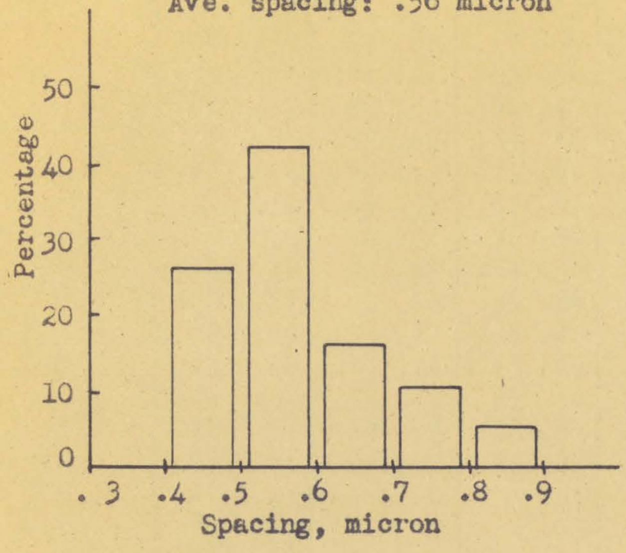

2. Tested statically
22 Spacing determinations
Ave. spacing: .52 micron

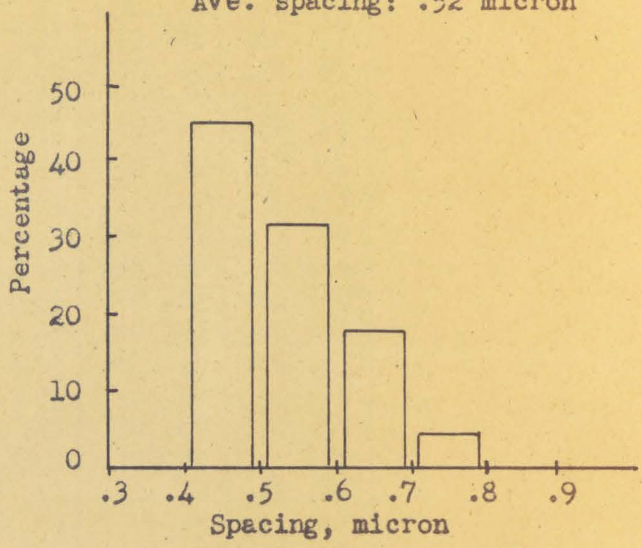

F. 1.3% Strain

1. Tested at 150 ft/sec
25 Spacing determinations
Ave. spacing: .54 micron

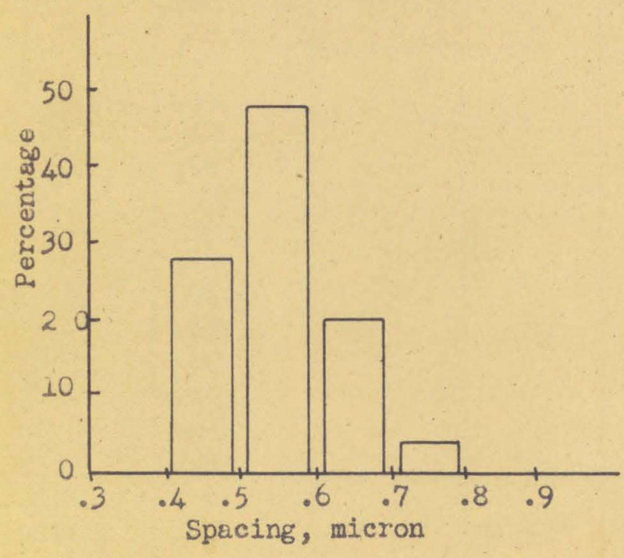

2. Tested statically
21 Spacing determinations
Ave. spacing: .59 micron

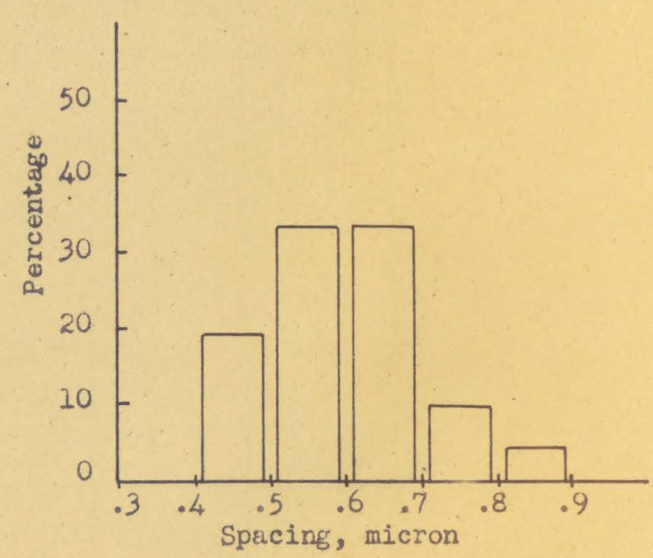

Table I
Slip Line Spacings (in microns) Observed in Individual Grains

Strain	10.9%		8.8%		6.6%		4.8%		2.4%		1.3%	
How Tested	Dyn.	St.	Dyn.	St.	Dyn.	St.	Dyn.	St.	Dyn.	St.	Dyn.	St.
	.87	.43	.81	.55	.43	.67	.48	.42	.58	.57	.62	.53
	.74	.57	.65	.70	.54	.40	.43	.69	.42	.47	.60	.71
	.67	.57	.91	.76	.73	.62	.59	.80	.56	.49	.72	.74
	.60	.55	.67	.80	.47	.60	.64	.52	.79	.48	.62	.57
	.71	.74	.76	.71	.60	.54	.47	.49	.49	.65	.54	.62
	.60	.61	.68	.53	.61	.49	.47	.59	.69	.59	.53	.62
	.89	.88	.85	.62	.54	.57	.53	.54	.49	.57	.49	.48
	.83	.54	.54	.99	.73	.64	.64	.56	.51	.42	.61	.56
	.57	.57	.85	.57	.67	.67	.76	.57	.61	.45	.57	.55
	.80	.70	.56	.72	.56	.71	.46	.64	.54	.47	.59	.59
	.88	.45	.83	.62	.54	.38	.39	.62	.56	.50	.56	.64
	.88	.77	.61	.60	.56	.56	.45	.67	.48	.53	.46	.48
	.66	.89	.59	.72	.66	.49	.39	.69	.48	.45	.55	.49
	.83	.56	.45	.74	.73	.59	.48	.59	.80	.48	.46	.63
	.88	.58	.59	.72	.59	.54	.50	.55	.56	.51	.55	.49
	.78	.61	.67	.77	.88	.53	.53	.46	.54	.67	.54	.69
	.77	.65		.62	.79	.68	.58	.65	.77	.70	.45	.80
	.61	.55		.60		.65	.60	.51	.51	.54	.48	.61
	.70	.59		.69		.53	.55	.53		.45	.53	.67
	.54	.68		.57		.61	.62	.53		.49	.41	.51
	.53	.71		.66		.54	.57	.67		.65	.69	.59
	.88	.71		.63		.61	.64	.54		.64	.53	
Slip	.55	.71		.81		.54	.43	.59			.52	
Line	.54	.65		.61		.57		.70			.43	
Spacings	.54	.57		.54		.77		.54			.53	
in	.67	.63		.70				.68				
Grains	.51			.64				.47				
Observed	.69			.73								
	.77			.80								
	.55			.47								
	.48			.67								
	.60			.84								
	.50			.87								
	.77											
	1.10											
	.64											
	.53											
	.67											
	.67											
	.66											
	.82											
	.60											
	1.10											
	.62											
	.81											
Ave. Spacing	.67	.62	.67	.67	.60	.56	.51	.57	.56	.52	.54	.59

Table II
General Comparison of Slip Line Characteristics

Strain, %	How Tested	No. of Grains Counted	Grains with Slip Lines		Grains with Lines too Fine to Resolve		Grains with Two Slip Systems		No. of Spacing Determinations	Ave. Spacing
			No.	Pct.	No.	Pct.	No.	Pct.		
10.9%	Static	154	153	99.5%	39	25.6%	74	48.0%	27	0.62
	Dyn.	123	123	100%	29	23.6%	54	43.9%	45	0.68
8.8%	Static	155	153	98.8%	30	19.4%	75	48.3%	33	0.67
	Dyn.	107	105	98.1%	38	36.1%	37	35.2%	16	0.67
6.6%	Static	192	192	100%	69	36.0%	74	38.5%	25	0.56
	Dyn.	100	97	97.0%	28	28.0%	53	53.0%	17	0.60
4.8%	Static	196	196	100%	60	30.6%	85	43.4%	27	0.57
	Dyn.	122	121	99.2%	48	39.4%	46	37.7%	24	0.51
2.4%	Static	157	157	100%	56	35.6%	80	51.0%	23	0.52
	Dyn.	107	104	97.3%	50	46.7%	38	35.5%	18	0.56
1.3%	Static	168	161	95.9%	101	60.1%	69	41.0%	22	0.59
	Dyn.	209	205	98.1%	121	57.9%	96	45.9%	23	0.54

have had only two systems acting, but because of the influence of the strain in a neighboring grain, another system of slip was induced to action near the boundary of the two grains.

There were some other results observed which cannot be expressed quantitatively. The first and most important is the difference that could be observed as the strain was increased. There is obviously a difference in the structure, although the above data do not reflect this fact. With more strain, it was observed that the surface of the specimen became more and more distorted. This fact is reflected in Figs. 10, 11, 12, photomicrographs showing regions with different strains. As the strain increased, it became more difficult to focus the metallograph on the surface, and a greater percentage of the area was blurred in the resulting picture. Also with increasing strain it was observed that the slip lines in those grains where the lines could be counted appeared darker and wider, indicating that greater amounts of strain had taken place on those planes. However, this fact was not reflected in the percentage of grains in which the lines were too indistinct to count.

Fig. 10- Strain: 2.4%
Impact Velocity: 150 ft/sec

Fig. 11- Strain: 4.8%
Impact Velocity: 150 ft/sec

Fig. 12- Strain: 8.8%
Impact Velocity: 150 ft/sec

Figs. 10, 11, 12 Show the Increasing Distortion of the Surface of the Material as the Strain is Increased. Magnification: 150x

CONCLUSIONS AND DISCUSSION

A. Conclusions

From the results obtained, it may be concluded that there is no microscopically observable difference in the microstructure resulting from the two different methods of testing, when the structures are compared on the basis of the same strain produced at each rate of loading. Although only one velocity of impact was employed (150 ft/sec) it is highly doubtful that other slower rates of loading would produce any different microstructure. The velocity used was the highest obtainable with the equipment at hand. It is also doubtful that higher strains would show any significant difference. The only possibility lies in strains in which the slip lines first begin to appear. It was found that strains less than 1.3 percent could not be produced with this equipment at the velocity employed.

It may also be concluded that except for the expected fact that with increasing amounts of strain, the slip lines are more distinct because of more slip on each individual slip plane, there is no observable dependence of the resulting microstructure on the amount of strain, in the range of strains from 1.3 percent to 10.9 percent. Although the percentage of total grains with slip lines was slightly higher for the larger strains, the percentage was so close to 100 percent in all cases that this is not a significant difference. One interesting fact is that the percentage of grains with more than one acting slip system did not change with increasing strain. It would be expected that in grains of this type first one slip system would appear, and with increasing strain another system would appear, producing a crisscross pattern of lines with the first system. But apparently if the grain is to have two systems of slip at a considerable amount of strain, both these systems appear in the grain at a very small amount of strain.

No conclusions could be made with respect to twinning, since if any twins are produced mechanically, they are so small that they are not detectable with the method of examination employed. It is certain, however, that no large mechanical twins are produced by either static or dynamic testing of alpha brass.

B. Discussion

For a more exacting analysis of the microstructure produced by plastic strain, more elaborate methods of inspection must be employed. Since the question of mechanical twinning in this material is still a controversial issue, it would be an interesting problem to check the work of Samans (4), by employing his method of analysis. Unfortunately this would not immediately answer the question as to whether there is also mechanical twinning produced in polycrystalline alpha brass, but it would shed some light on the subject.

The electron microscope would also be very useful in a more complete analysis of the resulting microstructure. Since this instrument has a much greater depth of focus than a visual microscope, areas which have very much distortion could be more completely analysed. During the course of this investigation, it was quite often observed that near a corner of a grain, instead of having less distortion because of the rigidity of the grain boundaries, the grain would be very distorted and have a very intense slip line distribution. Because of the distortion, this region could not be photographed, but with electron microscope little difficulty would be encountered in obtaining a photomicrograph which would help in the analysis of why there is so much distortion in this region.

There is one great deficiency in all the observations of microplastic strain by any present method. This is the impossibility of analysis of the influence of the surrounding grains on the grain under observation. Since there is no method of observing what happens under the surface, and since the surface that is observed is a free surface without the restraints that are present in the interior of the specimen, it is not possible to explain the actual causes of the resulting microstructure by the observations of the surface. For example, in many grains there appear isolated regions in which there are groups of slip lines having orientations and appearances different from the rest of the lines in the grain. Undoubtedly this is due to the action of another grain exerting a localized stress on a part of the hidden surface of the grain under observation, the effect being transmitted up through the grain to the free surface where it is observed. But the details of how much local distortion there is in the grain causing the appearance of these isolated groups of slip lines, the grain boundary conditions, the restraints of the surrounding grains, and why the pattern observed appears as it does are questions that cannot be answered.

REFERENCES

1.	C. S. Barrett	"Structure of Metals"	McGraw-Hill, New York (1943)
2.	C. F. Elam	"The Distortion of Metal Crystals"	Oxford, New York, (1935)
3.	C. H. Mathewson	"Twinning in Metals"	Trans. AIME, 78, 554, (1928)
4.	C. H. Samans	"X-Ray Study of Orientation Changes in Cold Rolled Single Crystals of Alpha Brass"	J. Inst. of Metals 55, 209, (1934)
5.	J. E. Burke and C. S. Barrett	"The Nature of Strain Markings in Alpha Brass"	AIME, T. P. No. 2327, (1948)
6.	R. G. Treuting and R. M. Brick	"Micrographic Observations of Slip Lines in Alpha Brass"	Trans. AIME, 147, 128, (1942)
7.	C. S. Barrett	"Metallography with the Electron Microscope"	Trans. AIME, 156, 62, (1944)
8.	R. L. Aston	Proc. Cambridge Phil. Soc.	23, 549, (1927)
9.	H. C. Mann	"High Velocity Tension Impact Tests"	Proc. ASTM, 36, 85, (1936)
10.	D. S. Clark and G. Dätwyler	"Stress-Strain Relations Under Tension Impact Loading"	Proc. ASTM, 38, 98, (1938)
11.	E. R. Parker and C. Ferguson	"The Effect of Strain Rate upon the Tensile Impact Strength of some Metals"	Trans. ASM, 30, 68, (1942)
12.	C. H. Mahtewson	"Structural Premises of Strain Hardening and Recrystallization"	Trans. ASM, 32, 38, (1944)
13.	C. A. Edwards	"The Resistance of Metals to Penetration Under Impact"	J. Inst. of Metals, 20, 77, (1918-22)

14.	C. H. Mathewson and K. R. van Horn	"Directed Stress in Copper Crystals"	Trans. AIME, 89, 59, (1930)
15.	E. N. Da C. Andrade and R. Roscoe	"Spacing of Glide Planes of Single Crystals of Lead"	Proc. Phys. Soc. (London), 49, 52, (1937)
16.	C. S. Barrett	"The Electron Microscope and Its Application To Metals"	Electronic Methods of Inspection of Metals, ASM (1947)
17.	V. K. Zworykin	"Applications of the Electron Microscope in Metallurgy"	Trans. AIME, 152, 13, (1943)
18.	E. R. Parker and E. A. Smith	"High Speed Tensile Impact Tests on Single Crystal and Poly-crystalline Copper"	AIME, T. P. 1704, (1944)
19.	P. E. Duwez, D. S. Wood, and D. S. Clark	"The Influence of Specimen Length on Strain Propagation in Tension"	N. D. R. C. Div.A, Sec. B, OSRD Contract OEM sr-348, Report No. 3
20.	T. H. von Kármán and P. E. Duwez	"On the Propagation of Plastic Strains in Solids"	Presented at Sixth International Congress for Applied Mechanics, Sept. 1946, Paris
21.	H. F. Bohnenblust, J. V. Charyk, and D. H. Hyers	"Graphical Solution for Problems of Strain Propagation in Tension"	N. D. R. C. Report No. A-131 (OSRD No. 1204)
22.	D. S. Clark, D. H. Hyers, D. S. Wood, and P. E. Duwez	"Mechanics of the Dynamic Performance of Metals"	N. D. R. C. Report No. M-385 (OSRD No. 4343)

APPENDIX I

Determination Of Theoretical Strain Distribution

The basis for the determination of the theoretical strain distribution is the von Kármán theory of plastic wave propagation.(20) From a consideration of forces and momentun in a prismatical bar subjected to longitudinal impact, the wave equation

$$\rho \frac{\partial^2 u}{\partial t^2} = T \frac{\partial^2 u}{\partial x^2}$$

was formulated. In this equation ρ is the mass density of the material, u is the displacement of a crossection from its original position x from the end of the bar that is struck, t is the time, and T is the slope of the stress-strain curve, $\frac{\partial \sigma}{\partial \epsilon}$. The strain as a function of x and t results from the equation $\epsilon = \frac{\partial u}{\partial x}$, where u, the solution of eq. (1), is a function of x and t.

From a development of the solutions of Eq. (1), it was shown (21) that a graphical solution of the resulting strain in a bar subjected to longitudind impact could be derived. The solution is developed (22) from a consideration of only the stress-strain curve for the particular material investigated, and the strain at any point in this particular bar is then dependent only on the velocity of impact, the position of the point under consideration along the bar, and the time since the end of the bar (x = o) was originally put in motion.

For the material used in this investigation, the stress-strain curve is shown in Fig. 13. For a graphical solution of the problem, the stress-strain curve must be approximated by a number of straight lines, and the degree of accuracy of the solution will depend on the accuracy of approximation of the stress-strain curve with these straight lines. These lines of approximation are shown in Fig. 13.

As a result of the stress-strain curve shown in Fig. 13, the $(c-\epsilon)$ curve, Fig. 14, is obtained. In this curve, c is the velocity of propagation of a plastic wave associated with the particular strain ϵ. This curve is obtained as a result of the equation

$$c = \sqrt{\frac{\frac{\partial \sigma}{\partial \epsilon}}{\rho}} = \sqrt{\frac{T}{\rho}}$$

which is another result of the von Kármán theory.

From the equation

$$v_i = \int_0^{\epsilon_i} \sqrt{\frac{T}{\rho}}\, d\epsilon$$

or simply a graphical integration of the $(c-\epsilon)$ diagram from $\epsilon = 0$ to $\epsilon = \epsilon_i$, the velocity v_i required to produce the strain ϵ_i near the moving end of the specimen is obtained.

The $(\sigma - v)$ diagram, Fig. 15, is now obtained from a plot of the velocity required to produce a strain ϵ_i near the moving end of the specimen and the stress σ_i associated with that same strain. The $(\sigma - v)$ diagram is obtained as a series of straight lines, but is approximated by a mean smooth curve. Then this $(\sigma - v)$ curve is again approximated by another series of straight lines, Fig. 16. In this approximation, the velocity of impact

v_i to be used in the actual test is chosen as an integral multiple of one half the velocity required to produce the maximum elastic strain, ϵ_o.

The procedure outlined in (Ref. 23) is now followed in obtaining the rest of the construction of Fig. 16. The (x-t) diagram, Fig. 17, may now be constructed, each region in this diagram representing a different amount of strain. The x coordinate in this diagram represents the distance along the specimen from the moving end, and the t coordinate represents the time elapsed since the end of the specimen was initially struck.

From the (x-t) diagram, the strain distribution at time t_i results directly since each region in this diagram corresponds to a point in the $(\sigma-v)$ diagram. The point in the $(\sigma-v)$ diagram is associated with a definite stress and hence a definite strain.

At time t_1 the strain distribution appears as in Fig. 18. If the impact is stopped after this time has elapsed, the resulting strain distribution should be as shown. Since only 9 lines were used to approximate the $(\sigma-v)$ diagram, the strain distribution appears as a series of 9 discrete values of strain; for a closer approximation to the resulting strain distribution, smaller intervals should have been chosen on the $(\sigma-v)$ curve. There are several justifications for the approximations used. One is the fact that the static stress-strain curve was used in the calculation, whereas it is known that the stress-strain curve is quite different under impact conditions. Secondly, the theory assumes that the moving end of the specimen may be instantly accelerated to the impact velocity, and that all parts of the impact testing machine are infinitely rigid; clearly neither of these conditions can be met in practice. Also since the original stress-strain curve was approximated as a series of straight lines the whole procedure was only an approximation.

Beginning with the actual stress-strain curve, applying a velocity of impact of 150 ft/sec in the calculations, and choosing t_2 to be the time during which the lower end of the specimen could travel at 150 ft/sec before the impact was stopped, the theoretical strain distribution appears as in Fig. 19. The actual test under these same conditions resulted in the dotted curve appearing in Fig. 19.

Table III
Static Test Data Obtained for Stress-Strain Curve

Load lb	Elongation in 7.74 in.	Strain %	Stress lb/in.^{2}	Load lb	Elongation in 7.74 in.	Strain %	Stress lb/in.^{2}
0	.000	.000	0	1062	1.000	12.92	31300
57	.0005	.010	1680	1074	1.050	13.57	31700
91	.001	.015	2680	1089	1.100	14.20	32100
142	.0015	.019	4190	1102	1.150	14.85	32500
196	.002	.026	5840	1120	1.200	15.50	33000
241	.0025	.032	7100	1148	1.300	16.80	33800
296	.0035	.045	8730	1170	1.350	17.42	34500
345	.004	.052	10180	1180	1.400	18.10	34800
395	.005	.065	11650	1196	1.450	18.73	35200
446	.006	.077	13170	1214	1.500	19.40	35800
494	.007	.090	14560	1244	1.600	20.6	36700
525	.009	.116	15480	1260	1.650	21.3	37200
542	.0125	.162	16000	1272	1.700	22.0	37500
553	.017	.220	16300	1285	1.750	22.6	37900
559	.0205	.265	16480	1295	1.800	23.2	38200
565	.0255	.330	16670	1306	1.850	23.9	38500
575	.0315	.407	16960	1324	1.900	24.5	39000
585	.040	.517	17260	1338	2.000	25.8	39500
592	.047	.607	17480	1348	2.050	26.5	39700
602	.057	.736	17760	1364	2.100	27.1	40200
610	.066	.853	18000	1370	2.150	27.8	40400
617	.074	.956	18200	1376	2.200	28.4	40600
623	.083	1.073	18370	1385	2.250	29.1	40800
628	.093	1.202	18520	1395	2.350	30.4	41100
638	.115	1.487	19030	1401	2.400	31.0	41300
655	.125	1.615	19320	1413	2.450	31.6	41700
670	.144	1.860	19760	1419	2.500	32.3	41800
673	.159	2.055	19830	1433	2.600	33.6	42200
684	.172	2.220	20200	1439	2.650	34.2	42400
697	.189	2.44	20600	1451	2.700	34.9	42800
701	.207	2.67	20700	1460	2.750	35.5	43000
715	.226	2.92	21000	1461	2.850	36.8	43100
726	.244	3.15	21400	1475	2.900	37.5	43500
741	.267	3.45	21900	1475	2.950	38.1	43500
753	.290	3.74	22200	1477	3.050	39.4	43600
772	.320	4.14	22800	1483	3.100	40.1	43700
795	.369	4.76	23400	1488	3.150	40.7	43800
803	.400	5.17	23700	1502	3.200	41.3	44200
823	.450	5.81	24200	1502	3.250	42.0	44200
848	.500	6.46	25000	1510	3.300	42.6	44500
873	.550	7.10	25700	1513	3.400	43.9	44600
900	.600	7.75	26500	1514	3.450	44.5	44600
921	.650	8.40	27200	1515	3.500	45.1	44700
942	.700	9.05	27800	1518	3.550	45.8	44700
981	.800	10.33	29000	1522	3.650	47.1	44900
997	.850	10.98	29400	1522	3.700	47.8	44900
1026	.900	11.63	30200	1530	3.800	49.0	45100
1041	.950	12.28	30700	1534	3.850	49.7	45200

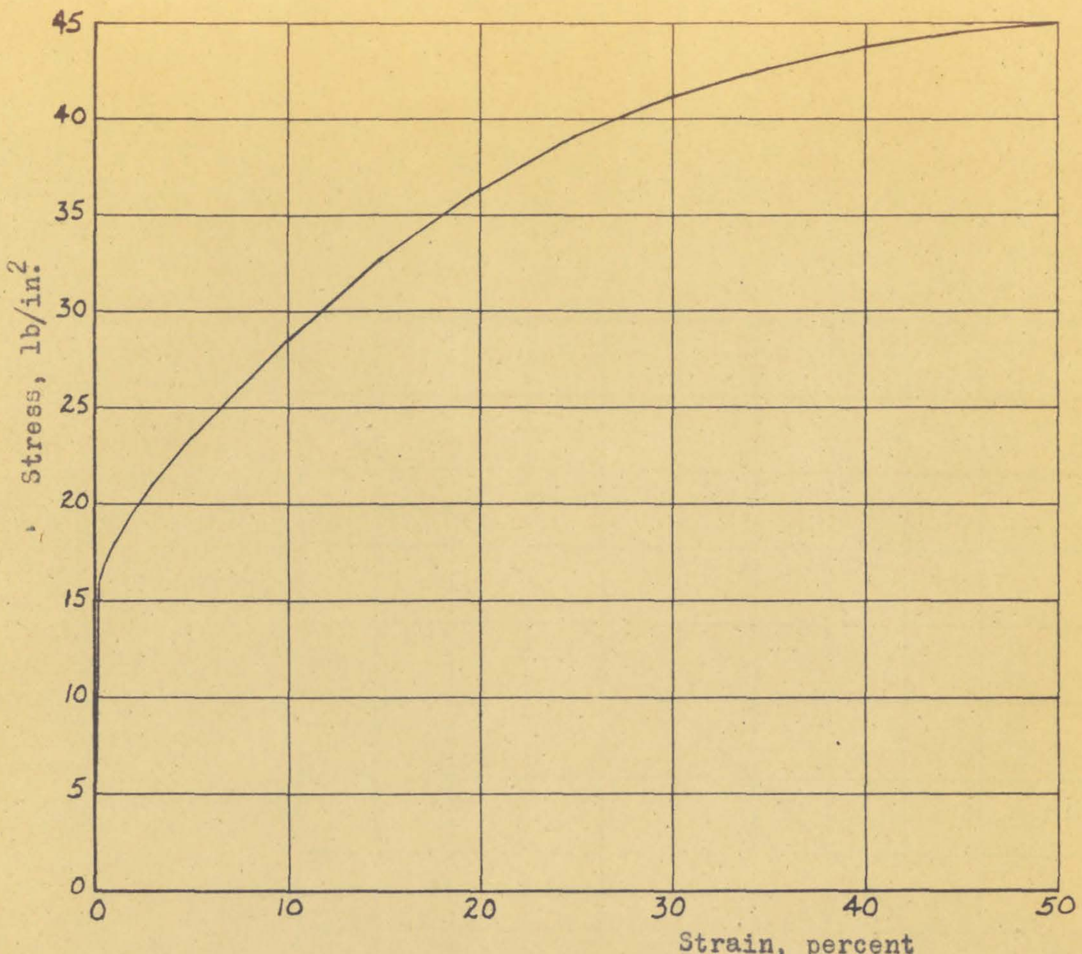

Fig. 13 Stress-Strain Diagram for Material Investigated

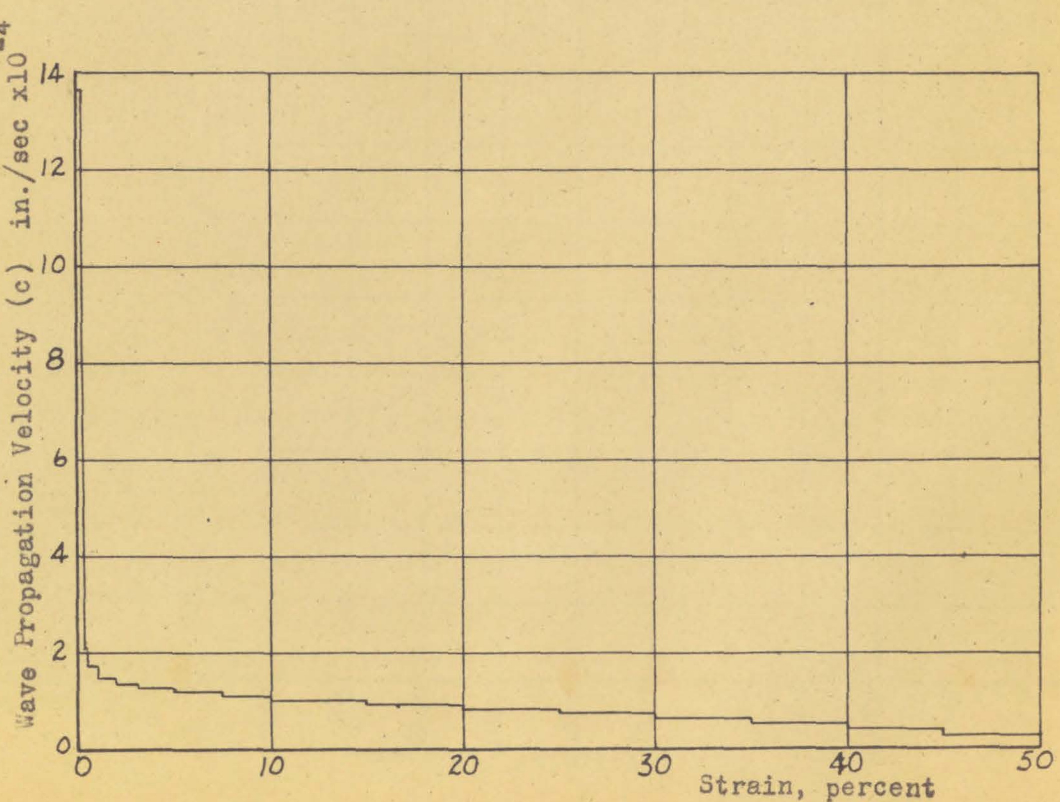

Fig. 14 (C- ∈) Diagram

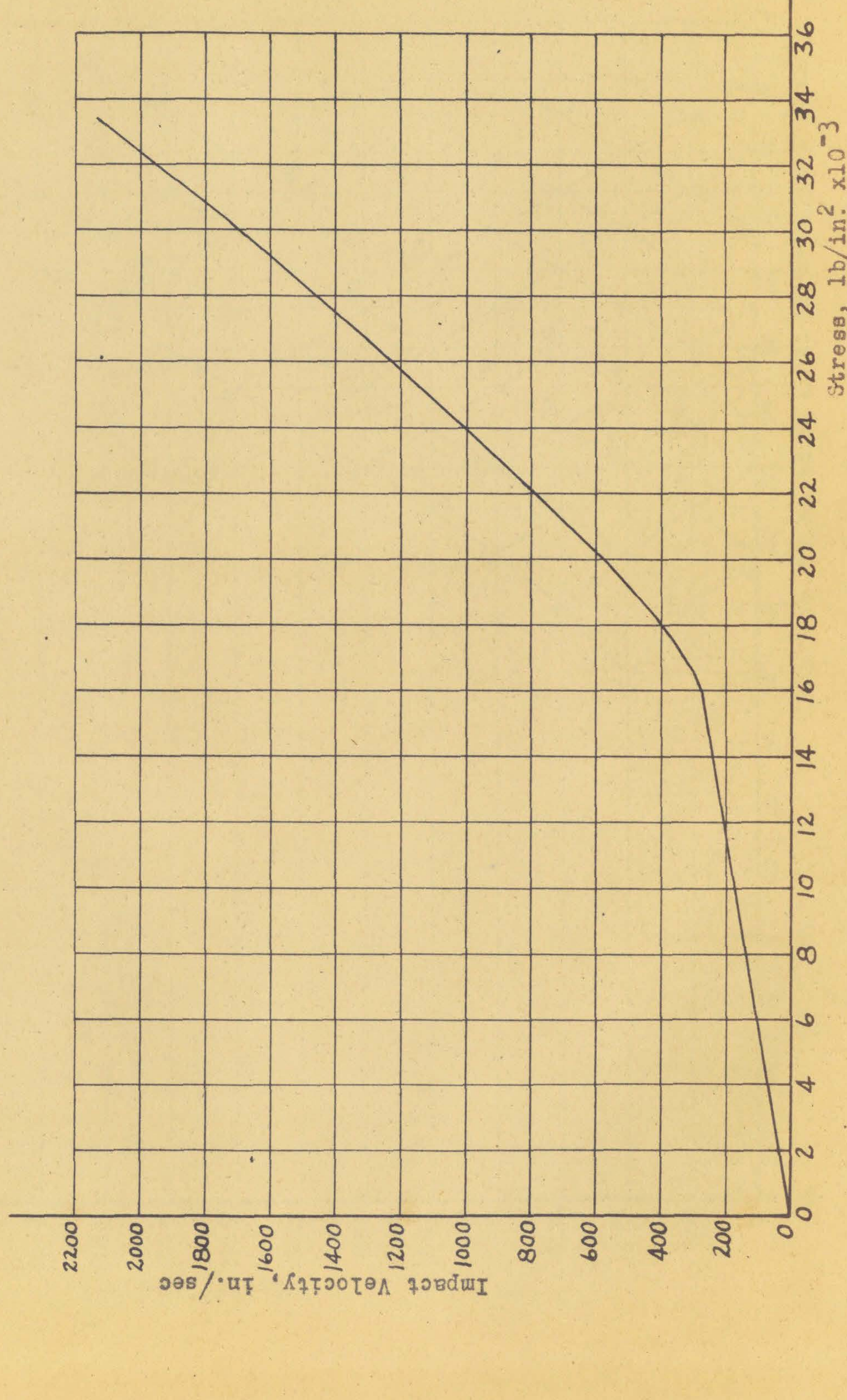

Fig. 15 Stress-Velocity Diagram

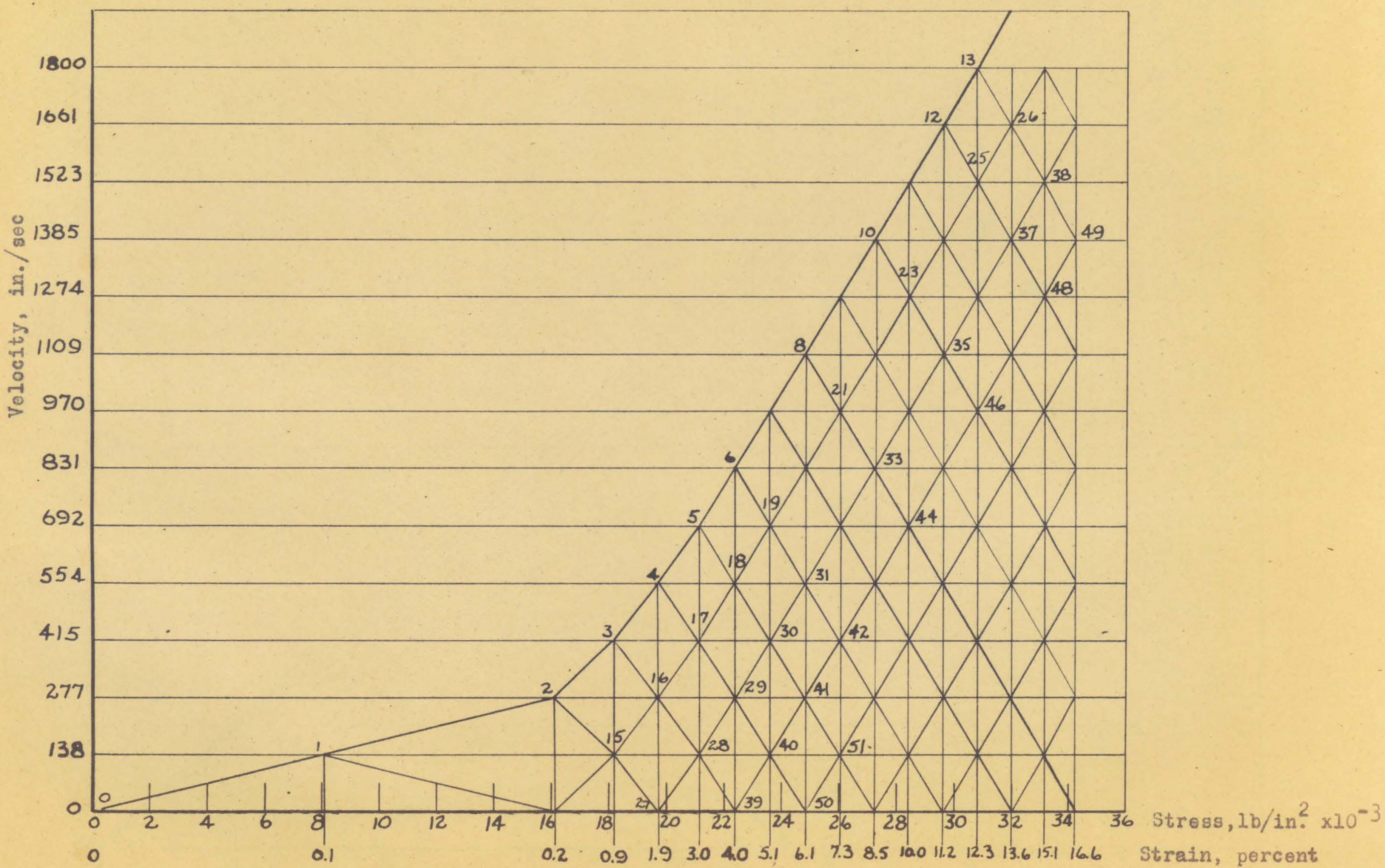

Fig. 16 Stress-Velocity Diagram

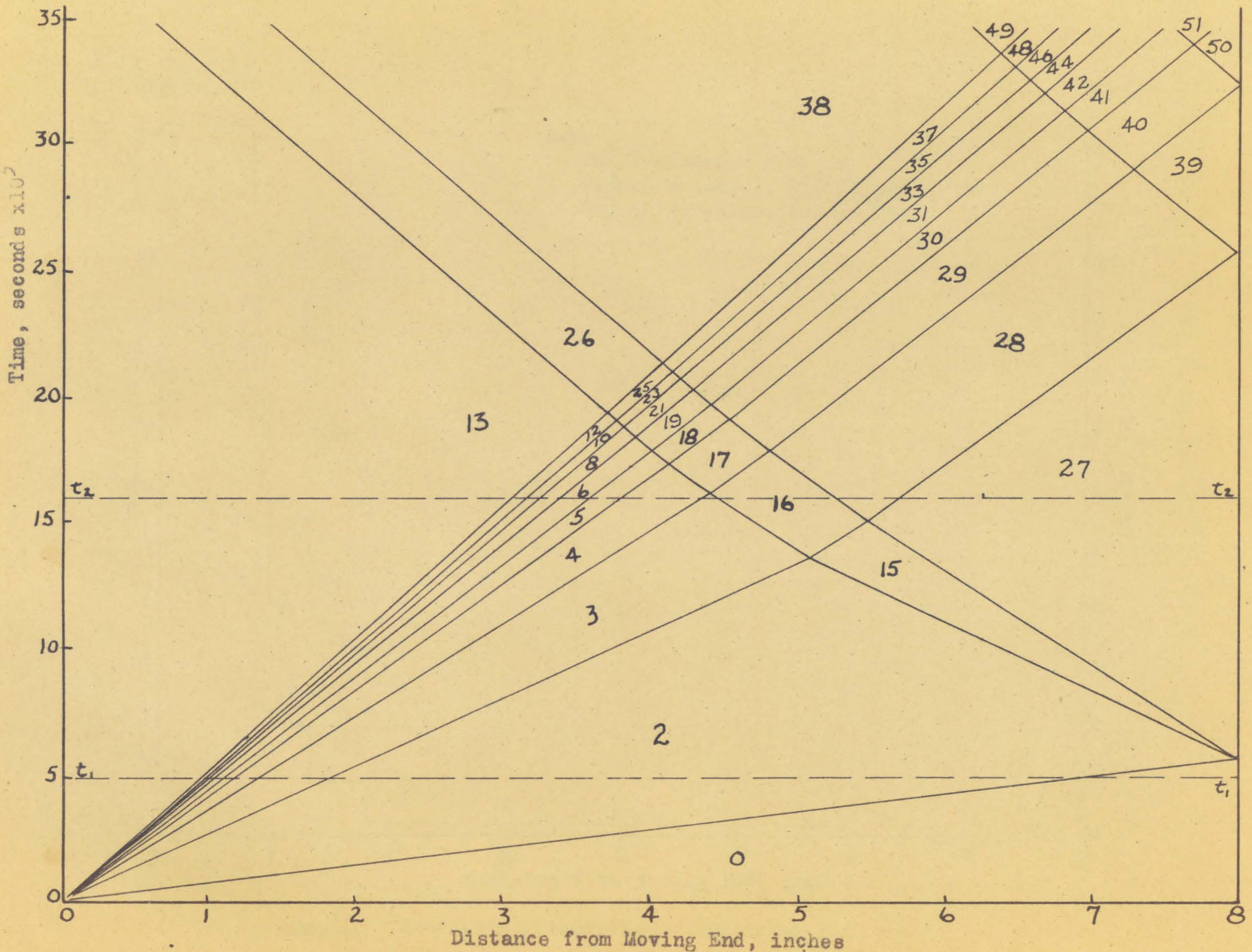

Fig. 17 (x-t) Diagram

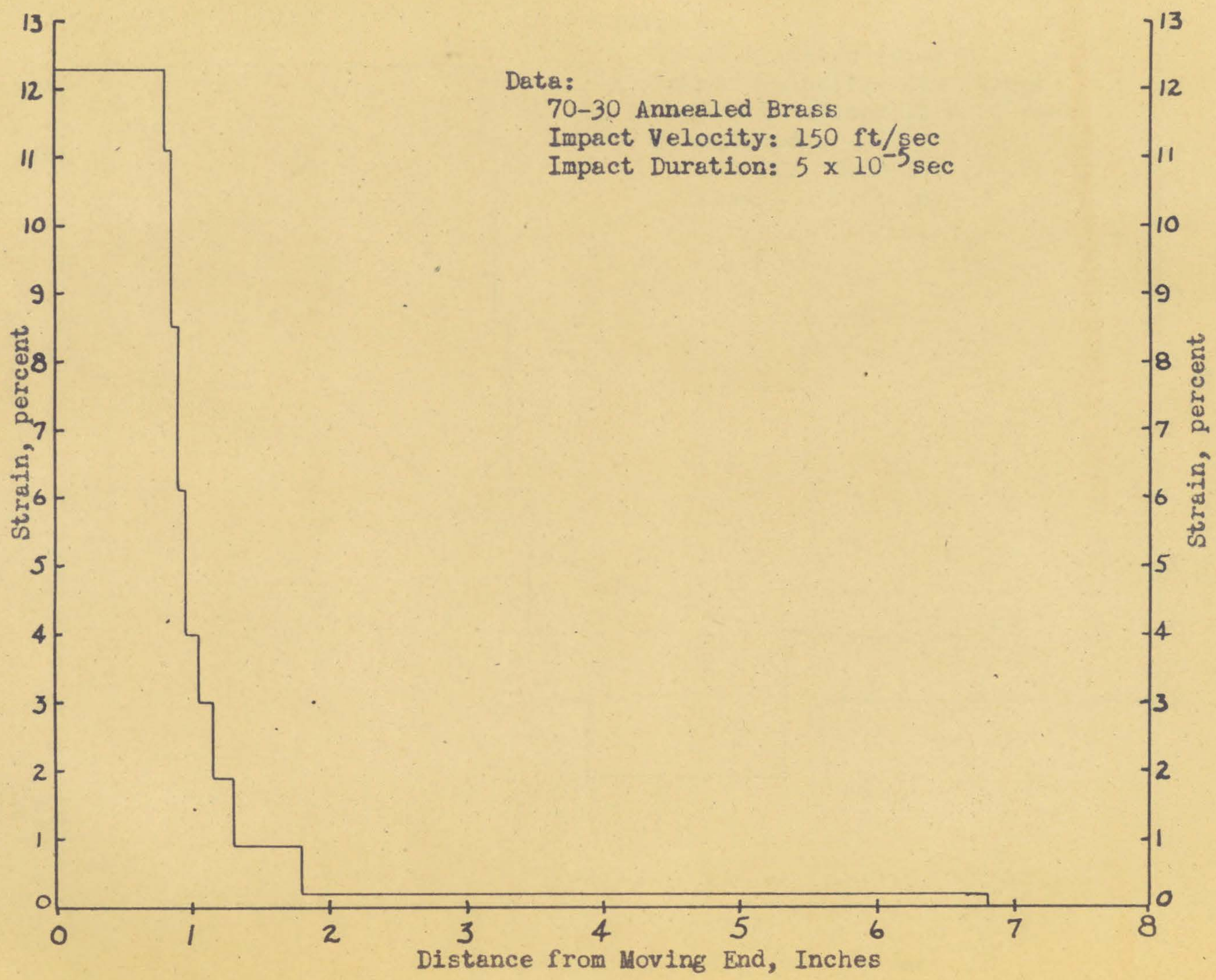

Fig. 18 Theoretical Strain Distribution at Time t_1

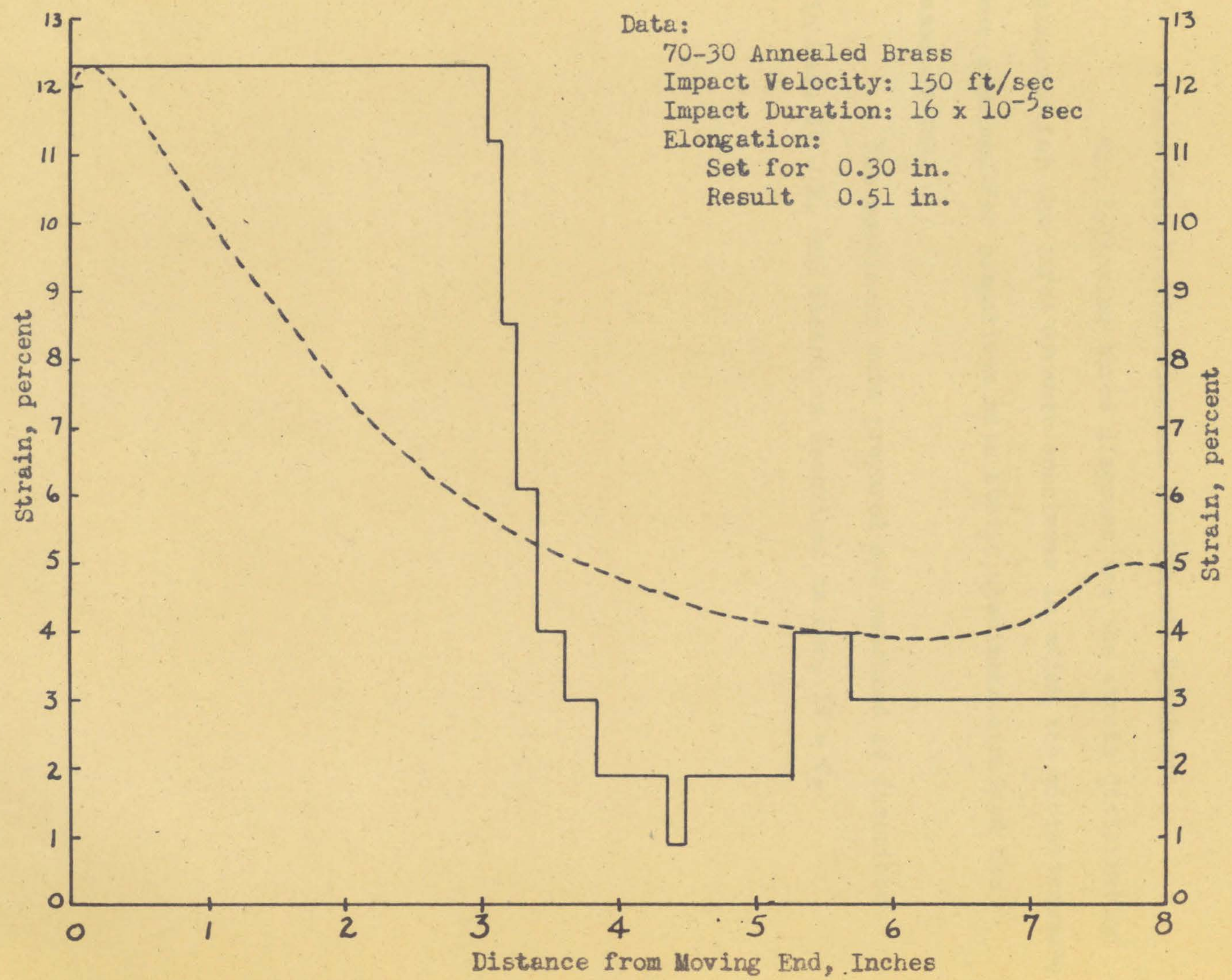

Fig. 19 Strain Distribution Diagram
Solid Diagram: Theoretically Predicted Strain Distribution
Dotted Curve: Actual Resulting Strain Distribution

APPENDIX II

Strain Distribution Diagrams For Dynamic Specimens

The following three diagrams are the strain distribution diagrams for the three dynamic specimens in which the microstructure was examined for comparison with static specimens strained the same amount.

The specimens were prepared and measured as described in Sec. IV - B, and tested as described in Sec. IV - C.

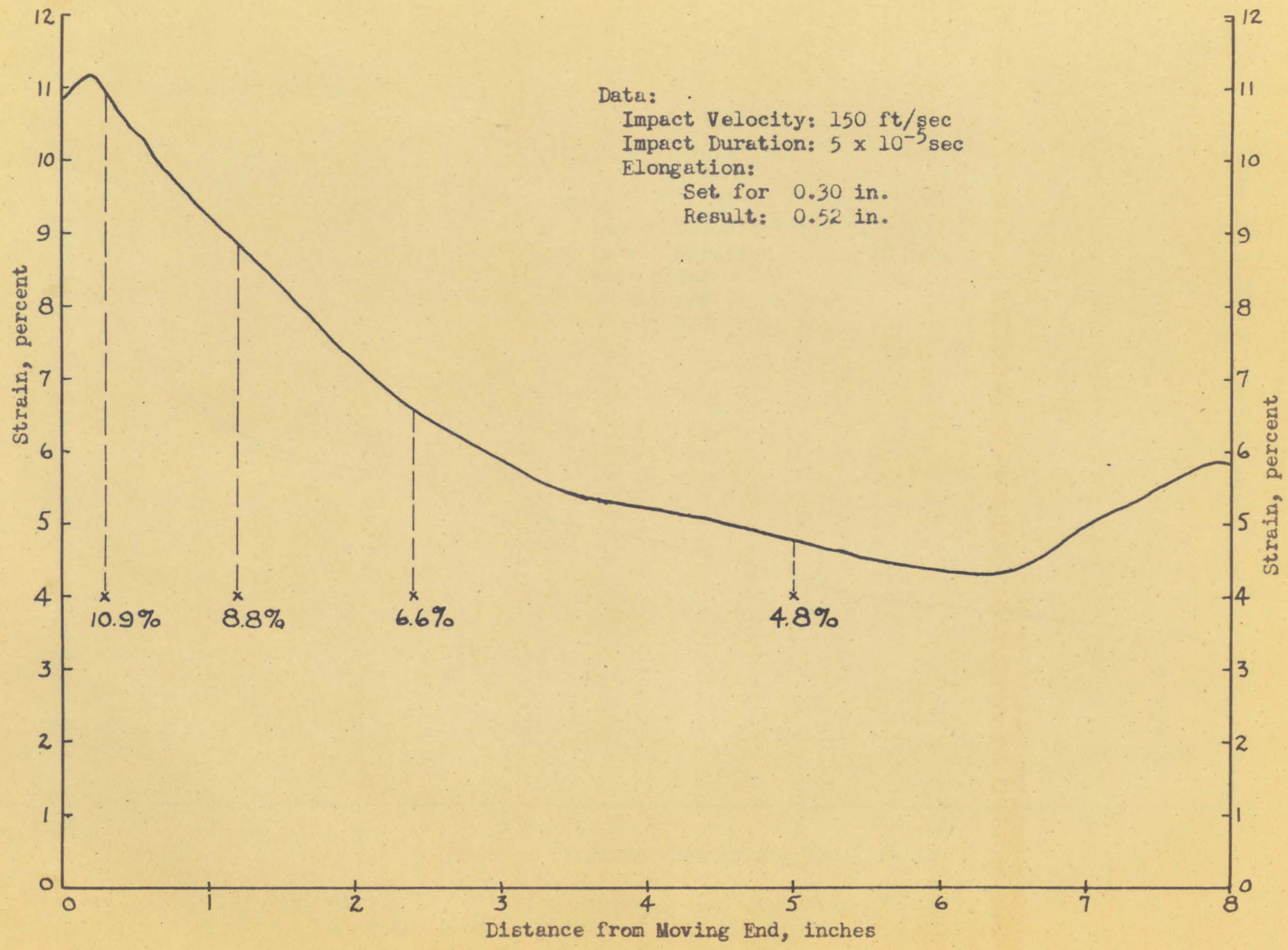

Fig. 20 Strain Distribution Diagram for a Specimen in which the Microstructure was Examined, and Indicating the Points at which the Examination was Made.

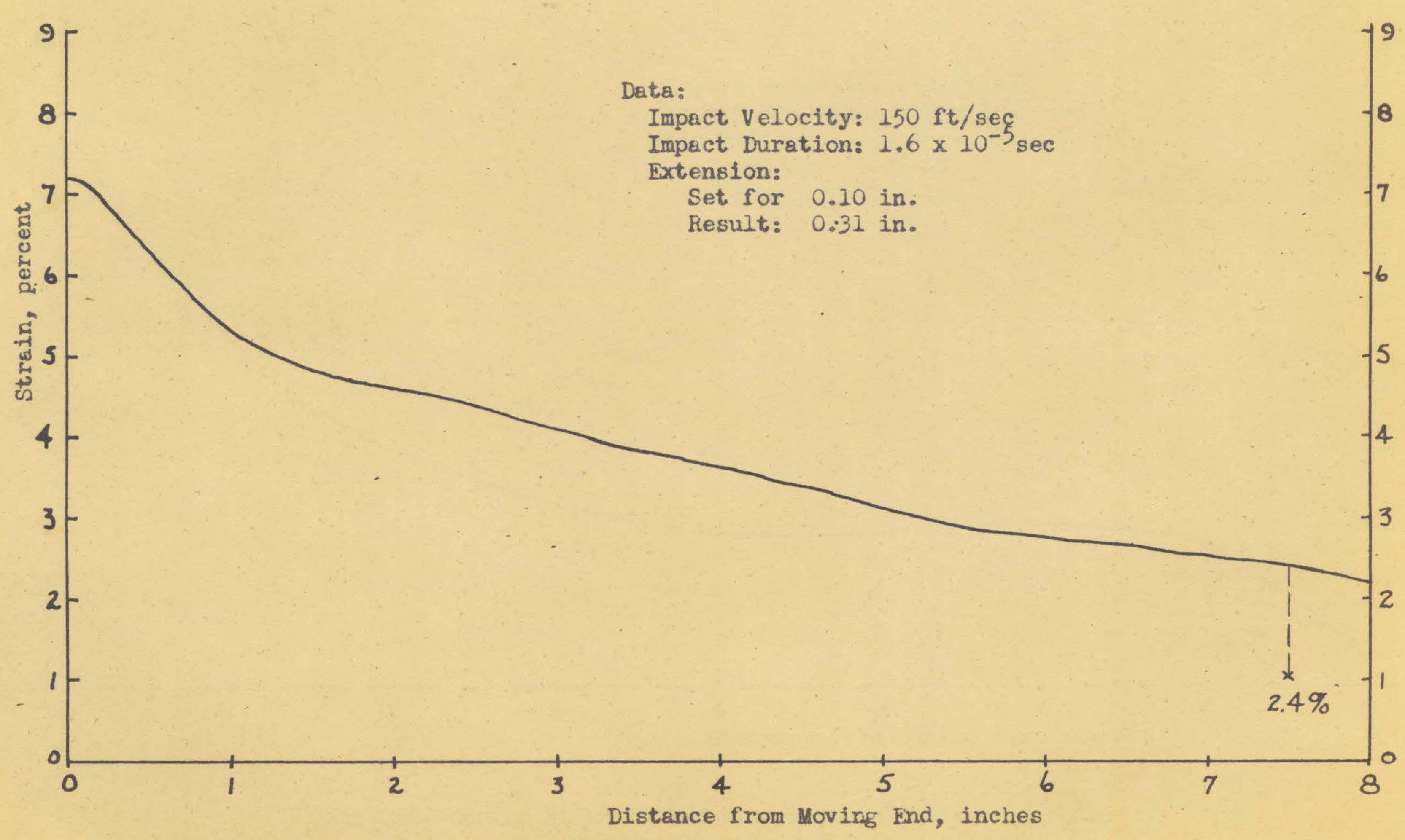

Fig. 21 Strain Distribution Diagram, and Indicating Point at which Dynamic Strain of 2.4% was Observed.

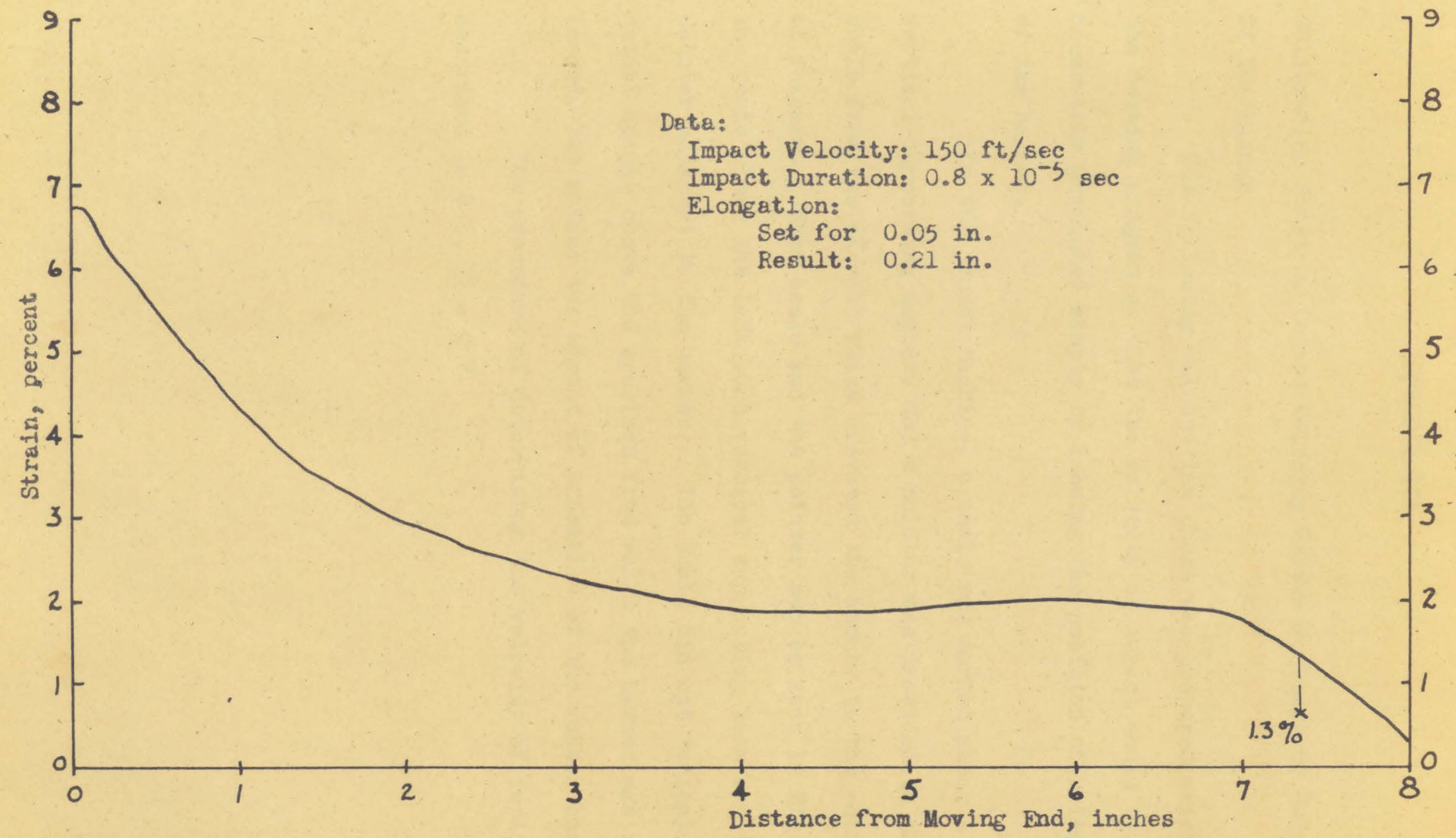

Fig. 22 Strain Distribution Diagram, and Indicating Point at which Dynamic Strain of 1.3% was Examined

APPENDIX III

Calibration Chart Of Impact Velocity Versus Position Of Release Of The Hammer

The following calibration chart was prepared prior to the testing program so that the velocity of impact could be accurately predicted simply by knowing the position of release of the hammer.

On the impact machine, a scale was marked along a vertical supporting member, and a pointer was provided to this scale from the element which elevated the hammer to the position of release. This scale and the pointer may be seen in Fig. 3, the scale along the left band vertical supporting beam and the pointer adjacent to the hammer. The scale did not indicate the actual height above the specimen from which the hammer was released, but rather the amount of extension of the rubber bands.

The procedure of determining the velocity of impact is described in Sec. IV - C 2.

Velocity Calibration Chart
Vertical Impact Testing Machine
Hammer: 3 3/4 lb
Propulsion:
6- 3/8 in. x 1 in. Rubber Bands